

Characterizing the non-monotonic behavior of mutual information along biochemical reaction cascades

Raymond Fan^{1,2} and Andreas Hilfinger^{1,2,3,4,*}

¹*Department of Physics, University of Toronto, 60 St. George St., Ontario M5S 1A7, Canada*

²*Department of Chemical & Physical Sciences, University of Toronto, Mississauga, Ontario L5L 1C6, Canada*

³*Department of Cell & Systems Biology, University of Toronto, 25 Harbord St, Toronto, Ontario M5S 3G5*

⁴*Department of Mathematics, University of Toronto, 40 St. George St., Toronto, Ontario M5S 2E4*

Cells sense environmental signals and transmit information intracellularly through changes in the abundance of molecular components. Such molecular abundances can be measured in single cells and exhibit significant heterogeneity in clonal populations even in identical environments. Experimentally observed joint probability distributions can then be used to quantify the covariability and mutual information between molecular abundances along signaling cascades. However, because stationary state abundances along stochastic biochemical reaction cascades are not conditionally independent, their mutual information is not constrained by the data processing inequality. Here, we report the conditions under which the mutual information between stationary state abundances increases along a cascade of biochemical reactions. This non-monotonic behavior can be intuitively understood in terms of noise propagation and time-averaging stochastic fluctuations that are short-lived compared to an extrinsic signal. Our results re-emphasize that mutual information measurements of stationary state distributions of cellular components may be of limited utility for characterizing cellular signaling processes because they do not measure information transfer.

INTRODUCTION

Cells respond and adapt to changing environments by transmitting information through biochemical reaction networks. A quantitative framework for analyzing this process is information theory, which was originally developed in the context of telecommunications [1] but has recently been applied to various biological problems such as determining the amount of information encoded in genes during fruit fly development [2] and deriving fundamental limits on the suppression of molecular fluctuations [3].

In biochemical reaction networks, information is transmitted through the time-varying concentrations of molecules [4–8]. Mutual information between temporal trajectories obeys the data processing inequality which establishes how information can only be lost but never recovered along communication channels [9]. This key theorem has been applied to derive constraints on noise suppression in cells [3] and a theoretical analysis of intracellular trajectories has characterized the information transfer through biochemical network motifs [6]. However, for cellular pathways it is practically impossible to directly estimate mutual information between trajectories from experimental data [10]. Recent work has thus focused on estimating the mutual information between trajectories indirectly through model simulations [4, 11, 12].

In contrast, the probability distributions of molecular abundances across a population of cells are directly experimentally accessible and are commonly reported to summarize the non-genetic variability of molecular abundances [13–15]. While such distributions are a powerful tool to analyze and describe stochastic fluctuations in cells [16], the mutual information between variables in

such distributions does not measure information transfer and is not constrained by the data processing inequality. The premise of the data processing inequality requires that a component becomes independent of an upstream signal when conditioned on an intermediate which is not the case for stationary state molecular levels in biochemical reaction cascades. Components in reaction cascades only become independent when conditioned on the entire histories of the intermediates [17–19].

Although the premise of the theorem is not satisfied, the data processing inequality has been incorrectly stated or implied when discussing stationary state distributions [20–23]. To counter these claims, recent work has reported that the mutual information between a signal and downstream components increases in the special case of a biochemical cascade with components of equal lifetimes and increasing average abundances [24, 25].

Here, we establish general conditions under which the mutual information between stationary distributions of components increases along simple biochemical cascades. Combining exact numerical simulations over a wide range of parameters with analytical approximations, we show that in a three variable linear cascade both inequalities implied by the data processing inequality will be violated when a slow read-out component averages out fast fluctuations of a noisy intermediate that responds to a slow extrinsic signal. This result contradicts the naive expectation that as long as the timescale of a signal is much slower than the timescales of the reaction network the mutual information between stationary state abundances decrease along biochemical cascades. We further show that this non-monotonic behavior is not special to linear cascades but also occurs in more complex reaction systems such as kinetic proofreading.

* andreas.hilfinger@utoronto.ca

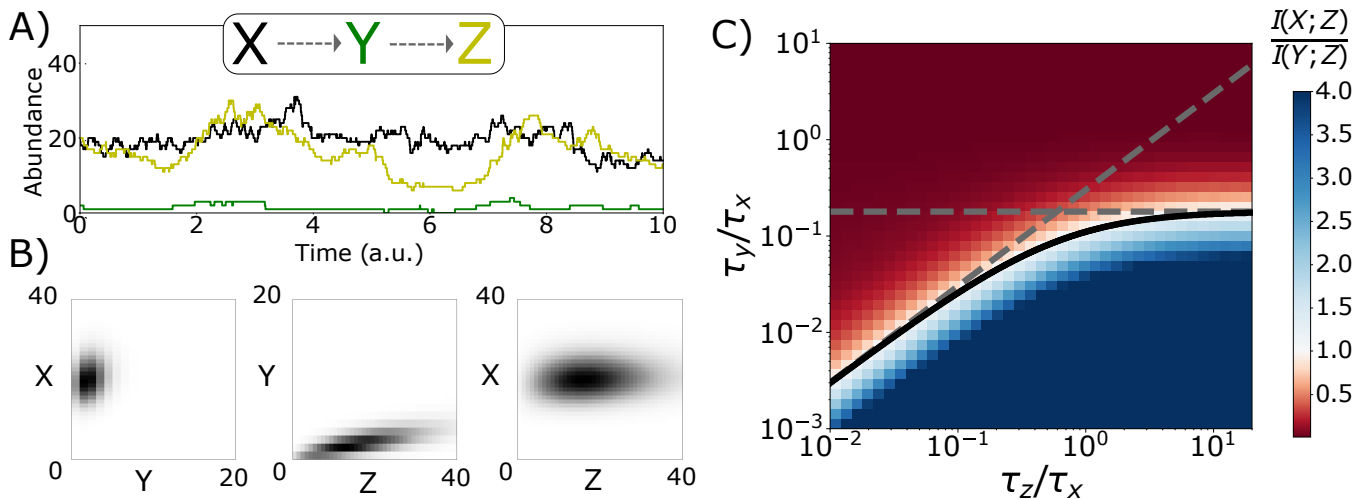
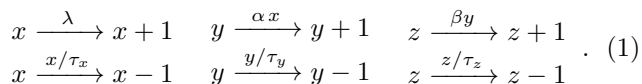


Figure 1. **The stationary state distributions of molecular abundances in biochemical cascades are not constrained by Eq. 2.** A) Example time trace of the linear cascade defined in Eq. 1 in which a signal X affects the production of Y , which in turn affects the production of Z . B) Corresponding stationary state distribution of molecular abundances. C) Exact numerical simulation results for the mutual information between pairs of variables in the stationary state distribution of the cascade defined by Eq. 1. The blue region indicates the regime in which the stationary state abundance of the final read-out component exhibits a lower mutual information with the intermediate of the cascade than with the further removed upstream signal. The solid black line indicates the analytical condition of Eq. 4 that approximately determines the boundary at which $I(X;Z) = I(Y;Z)$. Dashed grey lines indicate the approximate necessary (but not sufficient) conditions of Eqs. 6 and 7. The depicted results correspond to systems with average abundances $\langle x \rangle = \langle z \rangle = 20$ and $\langle y \rangle = 2$, representing a process with a noisy intermediate. Numerical simulations for other noise regimes show similar behavior, see supplement [26].

RESULTS

Mutual information is non-monotonic along biochemical cascades

To analyze mutual information in biochemical signaling we consider the following stochastic process in which three components X, Y, Z form a linear cascade



Here, variables linearly affect the production of the next downstream and each component undergoes first order degradation with respective average lifetimes τ_x, τ_y, τ_z .

The covariances between components of this generic regulatory cascade have been previously reported [27]. Here, we consider the joint stationary state distribution of molecular abundances $P_{ss}(x, y, z)$ and determine the mutual information [1] between pairs of abundances,

$$I(X;Y) := \sum_{x,y} P_{ss}(x,y) \log_2 \left(\frac{P_{ss}(x,y)}{P_{ss}(x)P_{ss}(y)} \right),$$

and analogously for any other pair.

The mutual information between pairs of components that form a Markov chain $X \rightarrow Y \rightarrow Z$ is constrained by the data processing inequality [9] which implies that

$$I(X;Z) \leq I(Y;Z) \quad (2)$$

$$I(X;Z) \leq I(X;Y). \quad (3)$$

This pair of inequalities establishes that information can only be lost along Markov chains and once information is lost it cannot be recovered through processing. However, while the biochemical cascade defined in Eq. 1 is Markovian in time, i.e., its future evolution depends only on the current state but not its history, the stationary state probability distributions of the process do not satisfy $P(X, Y, Z) = P(X)P(Y|X)P(Z|Y)$ [17–19] and are thus not constrained by the data processing inequality.

While this lack of conditional independence might look surprising, and has in fact been mistakenly assumed in related processes [20–23], it intuitively follows because Eq. 1 defines a dynamically varying stochastic process rather than a cascade of static random variables. In other words, the conditional probability distribution $P(Z|Y)$ is not entirely determined by how the dynamics of Z depends on Y but, e.g., depends on how long the system spends in each Y -abundance state which in turn depends on the abundance of X . The trajectories of abundances thus become conditionally independent only when conditioned on the temporal *history* of upstream variables [28–31].

We first analyze under which conditions the mutual information of the stationary state distribution of molecular abundances along the above biochemical cascade does not obey Eq. 2. Of course a proven theorem cannot be violated, but since the premise of the data processing inequality is not satisfied by the quantities under consideration they do not need to satisfy the theorem's conclusion. Using exact numerical simulations of the sys-

tem defined by Eq. 1 using the Gillespie algorithm [32] we find that for any tested molecular abundance levels, Eq. 2 was reversed in the regime when τ_z/τ_x is large and τ_y/τ_x is small as indicated by the blue region in Fig. 1B. In this regime the abundance of the intermediate component Y contains significantly less information about the abundance of the final read-out variable Z than the more distantly connected upstream signal X . See supplement [26] for numerical simulation results for abundances other than those depicted in Fig. 1B.

The above timescale dependence can be intuitively understood through approximate analytical arguments. For multivariate Gaussian distributions, the mutual information between components is related to their correlation through $I(X; Y) = -\log_2(1 - \rho_{xy}^2)/2$. When stationary state distributions are approximately Gaussian, we can thus estimate the mutual information between components from their correlations, which can be exactly determined from the system's chemical master equation, see Appendix A.

Following this approach yields the following (approximate) necessary and sufficient condition to reverse Eq. 2.

$$\begin{aligned} & 1 + \frac{\tau_y}{\tau_z} \left(1 + \frac{\eta_y^{\text{int}}}{\eta_{\text{sig}}} \left(1 + \frac{\tau_y}{\tau_x} \right) \right) \left(1 + \frac{\tau_z}{\tau_x} \right) \\ & \leq \left(1 + \frac{\tau_y}{\tau_z} \right) \left(\frac{\eta_y^{\text{int}}}{\eta_{\text{sig}}} + \frac{1}{1 + \frac{\tau_y}{\tau_x}} \right)^{1/2}, \end{aligned} \quad (4)$$

where we have introduced the normalized signal variability and intrinsic noise terms

$$\eta_{\text{sig}} := \frac{\text{Var}(x)}{\langle x \rangle^2}, \quad \eta_y^{\text{int}} := \frac{1}{\langle y \rangle}, \quad \eta_z^{\text{int}} := \frac{1}{\langle z \rangle}. \quad (5)$$

Here, and throughout angular brackets denote stationary state averages.

In Fig. 1C, the black line indicates the boundary defined by Eq. 4 which agrees well with the numerical solutions for the cascade defined in Eq. 1 with abundances $\langle x \rangle = \langle z \rangle = 20$, $\langle y \rangle = 2$ such that $\eta_y^{\text{int}}/\eta_{\text{sig}} = 10$. Eq. 4 also accurately describes systems with different variability ratios as long as the average abundances of all molecules are larger than one molecule [26].

The analytical condition of Eq. 4 can be intuitively understood in the regimes in which τ_z is much slower or much faster than τ_x . When $\tau_z \ll \tau_x$ the inequality asymptotically becomes

$$\sqrt{1 + \frac{\eta_y^{\text{int}}}{\eta_{\text{sig}}}} \leq \frac{\tau_z}{\tau_y}, \quad (6)$$

as long as $\tau_y \ll \tau_x$, see Appendix A2. Eq. 6 is indicated by the diagonal line of Fig. 1.

When $\tau_z \gg \tau_x$ the boundary asymptotically becomes a simple cutoff $\tau_y/\tau_x \lesssim \mu$ where μ is the root of a quintic polynomial in $\eta_y^{\text{int}}/\eta_{\text{sig}}$, see Appendix A2. While the

root is not analytically accessible we can calculate it numerically (see Fig. 2) and analytically determine its maximum value given by

$$\mu^* = \frac{\sqrt{2} - 1}{2} \approx 0.2071, \quad (7)$$

which is attained when $\eta_{\text{sig}} = (6 - 2\sqrt{2})\eta_y^{\text{int}}$, suggesting that violations of Eq. 2 will not be observed in systems in which the lifetime of the intermediate variable is larger than one fifth of the input signal regardless of noise levels and other timescales.

These asymptotic behaviors of Eq. 4 translate into a simple pair of necessary conditions on the timescales as indicated by the grey dashed lines in Fig. 1C. The mutual information between stationary state distributions of molecular abundances along a linear cascade is thus expected to violate Eq. 2 when a slowly varying signal affects a downstream component through a short-lived and noisy intermediate.

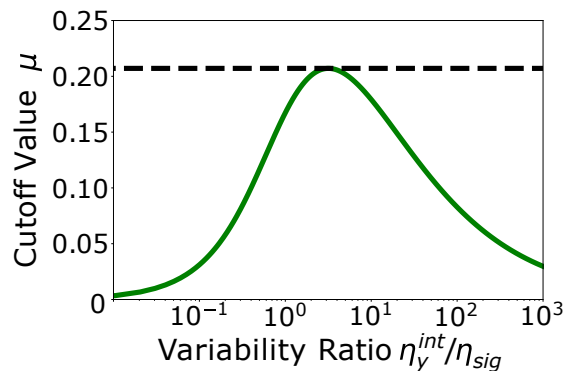


Figure 2. **Analytical approximations predict that Eq. 2 will not be reversed in cascades with a slow intermediate.** Eq. 4 predicts that violating Eq. 2 requires $\tau_y/\tau_x < \mu$ where the cutoff parameter μ depends on the variability ratio $\eta_y^{\text{int}}/\eta_{\text{sig}}$ and approaches zero in both limits. Dashed line indicates the analytically determined maximum of Eq. 7, which corresponds to the largest value of τ_y/τ_x for which violations of Eq. 2 are expected. Regardless of any other system details we thus do not expect violations in cascades with a relatively slow intermediate component.

The above results establish the conditions under which the mutual information between the last component and their upstream components can be non-monotonic, i.e., components that are further removed from the final read-out can have larger mutual information when compared to those closer connected to the final component. Next, we consider the complementary question when a seeming “loss of information” in the first step of the cascade will be recovered through an additional step, i.e., we analyze the conditions under which inequality Eq. 3 is violated.

Previous work [24, 25] established that this inequality will be violated when the signaling timescale is long-lived compared to downstream components with equal lifetimes and increasing abundances along the cascade. Next, we generalize those results to biochemical cascades with arbitrary timescales and abundances. For a given

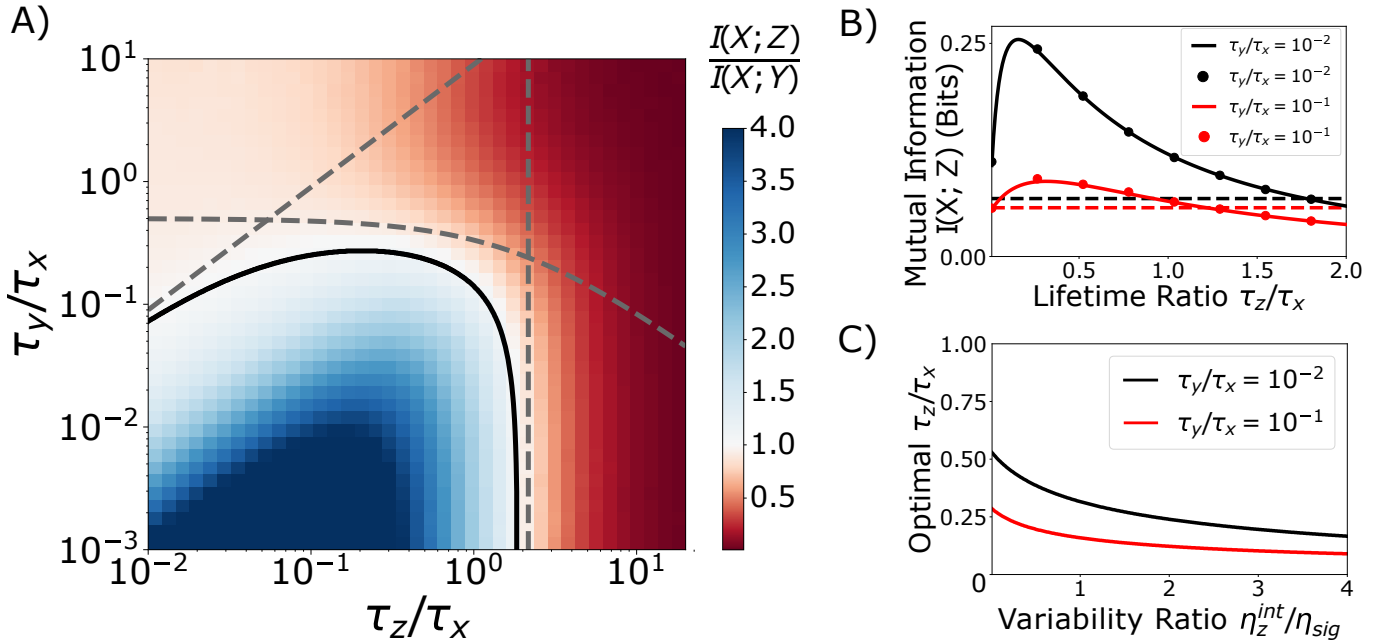


Figure 3. **Mutual information between stationary state abundances can increase along a biochemical cascade.** A) Exact numerical simulation results for the stationary state distributions of molecular abundances in the cascade defined by Eq. 1 with noise parameters as in Fig. 1. When the signal timescale is slowest in the cascade, and Y is fast compared to Z , the upstream signal exhibits a larger mutual information with the final read-out variable than with the intermediate as indicated by the blue region. The solid black line indicates the analytical approximation of Eq. 8 for the boundary at which $I(X;Z) = I(X;Y)$. Dashed grey lines indicate intuitively interpretable necessary (but not sufficient) conditions of Eqs. 9–11 for violations of Eq. 3 to occur. B) When keeping all other parameters fixed $I(X;Z)$ exhibits a maximum as a function of the relative timescale τ_z/τ_x . This maximum is significantly higher than $I(X;Y)$ (dashed lines) as long as the intermediate variable is sufficiently short-lived. C) In the regime in which an optimal lifetime ratio exists, it decreases monotonically as the variability ratio $\eta_z^{\text{int}}/\eta_{\text{sig}}$ increases, see Appendix A.1.

set of variability ratios the numerically observed behavior of the mutual information between stationary state abundances depends on the relative timescales of the system as indicated in Fig. 3A. Changing the variability ratios by adjusting average abundances affects the possible behavior significantly. For example, when the variability of the read-out variable was comparable to the intrinsic noise of the intermediate, we did not observe violations of Eq. 3 over the numerically explored timescales [26].

To understand this dependence we derive approximate analytical conditions under which the mutual information between molecular abundances increases along biochemical cascades. Following the same Gaussian approximation as above, we translate the exact (co)variance solutions for Eq. 1 into the following approximate condition for processes to violate Eq. 3

$$\begin{aligned} \frac{\left(1 + \frac{\tau_z}{\tau_x}\right)^2}{1 + \frac{\tau_y}{\tau_x}} \left(\frac{1}{1 + \frac{\tau_z}{\tau_y}} + \frac{1}{1 + \frac{\tau_y}{\tau_z}} \frac{1}{1 + \frac{\tau_z}{\tau_x}} \right) + \frac{\eta_z^{\text{int}}}{\eta_{\text{sig}}} \left(1 + \frac{\tau_z}{\tau_x}\right)^2 \\ \leq \frac{\eta_y^{\text{int}}}{\eta_{\text{sig}}} \left(1 - \frac{\left(1 + \frac{\tau_z}{\tau_x}\right)^2}{1 + \frac{\tau_z}{\tau_y}}\right) + \frac{1}{1 + \frac{\tau_y}{\tau_x}}. \end{aligned} \quad (8)$$

The boundary defined by Eq. 8 agrees well with the

exact numerical results for a system with variability ratios $\eta_y^{\text{int}}/\eta_{\text{sig}} = 10$ and $\eta_z^{\text{int}} = \eta_{\text{sig}}$, as indicated by the solid black line in Fig. 3A.

To intuitively understand the condition of Eq. 3 we first consider the maximum τ_z/τ_x above which violations become impossible. The exact cut-off value depends on both variability ratios (see supplement [26]) but is itself bounded by

$$\frac{\tau_z}{\tau_x} \leq \sqrt{\frac{\eta_y^{\text{int}}}{\eta_z^{\text{int}}}} - 1, \quad (9)$$

indicated by the vertical (dashed) grey line in Fig. 3. Note, Eq. 9 explains why violations of Eq. 3 were not observed in our numerical simulations when the read-out-variable was noisier than the intermediate [26].

Considering the regime in which $\tau_z, \tau_y \ll \tau_x$, leads to the following necessary condition

$$\frac{\tau_y}{\tau_z} \leq \frac{\eta_y^{\text{int}}}{\eta_z^{\text{int}}} - 1, \quad (10)$$

which illustrates that the read-out variable Z must become longer lived the closer its intrinsic noise gets to that of the intermediate in order for the mutual information to increase along the cascade. The condition of Eq. 10 is indicated by the diagonal dashed grey line in Fig. 3.

Finally, we consider the limit in which the intermediate component is far noisier than the others, i.e., $\eta_y^{\text{int}} \gg \eta_{\text{sig}}, \eta_z^{\text{int}}$. In this regime, Eq. 8 becomes independent of the variability ratios and constrains the timescales through

$$\frac{\tau_y}{\tau_x} \leq \frac{1}{2} \left(1 + \frac{\tau_z}{2\tau_x} \right)^{-1}. \quad (11)$$

indicated by the curved dashed grey line in Fig. 3. Because the right hand side of Eq. 11 is bounded by 1/2 it puts an upper limit on the lifetime of the intermediate variable for violations of Eq. 3 to occur. This suggests that an increase in mutual information between molecular abundances will not be observed in biochemical cascades in which the lifetime of intermediate variable is longer than one half of that of the input signal. Eqs. 9, 10, and 11 are derived in Appendix A 2.

While the above conditions are necessary but not sufficient they intuitively describe the qualitative behavior of the system: We conclude that the inequalities of Eqs. 2 and 3 are simultaneously reversed when the input signal X is the slowest component, the intermediate component Y is the fastest and contains more intrinsic noise than Z . In this regime, the mutual information between the components at the end of the cascade $I(X; Z)$ is larger than the mutual information between the abundance of either pair of directly connected components $I(X; Y), I(Y; Z)$.

How an additional ‘‘read-out’’ step can increase mutual information between molecular abundances can be intuitively understood in the regime in which the input signal varies on slower timescales than the lifetime of downstream cellular components, i.e., $\tau_x \gg \tau_y, \tau_z$ as is expected for many biological input signals. Under the above Gaussian approximation, the mutual information between X and Y is then given by

$$I(X; Y) = \frac{1}{2} \log_2 \left(1 + \frac{\eta_{\text{sig}}}{\eta_y^{\text{int}}} \right). \quad (12)$$

In contrast, the mutual information between X and Z is given by

$$I(X; Z) = \frac{1}{2} \log_2 \left(1 + \frac{\eta_{\text{sig}}}{\eta_z^{\text{int}}} \frac{1}{1 + \frac{\eta_y^{\text{int}}}{\eta_z^{\text{int}}} \frac{\tau_y}{\tau_x}} \right). \quad (13)$$

We see the magnitude of $I(X; Y)$ is limited by $\eta_{\text{sig}}/\eta_y^{\text{int}}$, while the magnitude of $I(X; Z)$ is limited by $\eta_{\text{sig}}/\eta_z^{\text{int}}$ when Z becomes slow. The additional read-out step thus performs time-averaging that effectively replaces the intrinsic noise of Y with that of Z . How much time-averaging is needed to violate Eq. 3 depends on the ratio of intrinsic noises as given by Eq. 10.

This suggests the increase in mutual information across more distant variables in a cascade occurs because the final slow variable filters out fast intrinsic noise of intermediates as previously reported for stochastic biochemical

reaction cascades [13, 27, 33, 34] Such time-averaging is common in biology and has, e.g., been reported in bacterial sensing [35]. It is equivalent to low-pass filters used in signal processing to remove high-frequency noise in engineering applications [36].

Optimal timescale for maximizing mutual information

The above results show that adding a component to a biochemical cascade can increase the mutual information between the stationary state abundances of the last component and the upstream input. Next, we determine the optimal timescale over which the additional variable Z should average out fluctuations to maximize $I(X; Z)$.

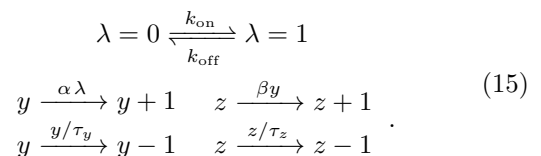
For distributions that are approximately Gaussian, we find for the ideal read-out variable with $\eta_z^{\text{int}} = 0$ the optimal timescale τ_z^* is given by

$$\tau_z^* = \tau_x \sqrt{\frac{\frac{\tau_y}{\tau_x} - 2 \left(\frac{\tau_y}{\tau_x} \right)^3 - \left(\frac{\tau_y}{\tau_x} \right)^2 \left(1 + 2 \frac{\eta_{\text{sig}}}{\eta_y^{\text{int}}} \right)}{\left(1 + \frac{\tau_y}{\tau_x} \right) \left(\frac{\eta_{\text{sig}}}{\eta_y^{\text{int}}} + \frac{\tau_y}{\tau_x} \right)}}. \quad (14)$$

The existence of this optimum can be intuitively understood because in the limit of $\tau_z \rightarrow \infty$, Z averages out both intrinsic fluctuations from the intermediate as well as the signal, see Fig. 3B. For read-out variables with finite noise, the optimal timescale τ_z^* monotonically decreases as η_z^{int} increases, see Fig. 3C, until ultimately violations of Eq. 3 are no longer possible for any value of τ_z , see Appendix A 1.

On-off upstream

Instead of a Poissonian input signal, we next consider a two-state input signal, e.g., motivated by a single receptor that is in a bound/unbound state, or by a gene stochastically switching between two transcriptional states. We thus analyze the following cascade in which the production rate of Y stochastically switches on and off according to



Exact numerical simulations of the process defined in Eq. 15 show that Eqs. 2, 3 are also violated in this strongly non-Gaussian biochemical cascade, see Fig. 4B. Note, the stochastic switching process of Eq. 15 yields identical mathematical forms for the covariances and correlation coefficients as the original model given by Eq. 1

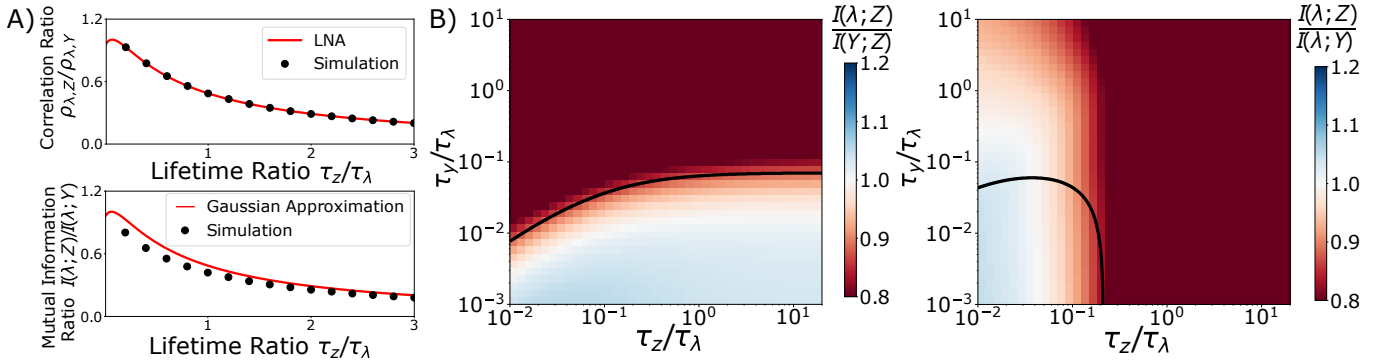


Figure 4. **Gaussian approximations make qualitatively correct but quantitatively inaccurate predictions for mutual information in cascades responding to on-off signals.** A) Comparing exact numerical simulations with analytical results for the cascade defined by Eq. 15. Correlation coefficients are exactly predicted by the linear noise approximation (LNA) because all rates are linear. Mutual information is only approximately predicted by Gaussian approximations. Data corresponds to a cascade with abundances $\langle y \rangle = 2$, $\langle z \rangle = 20$ and $\tau_y/\tau_\lambda = 0.1$, $P_{\text{on}} = 0.5$. B) Exact numerical simulations show the Gaussian approximation (black line) no longer quantitatively predicts the region of violations, but qualitative timescale features are accurately characterized, i.e., for noisy intermediates Eq. 2 is not obeyed when the intermediate Y is significantly faster than both X , Z , and Eq. 3 is not obeyed when the signal timescales are longer lived than all other components. Same parameters as panel (A).

with the only difference that variability of the input signal is now given by

$$\eta_\lambda = \frac{1 - P_{\text{on}}}{P_{\text{on}}}, \quad (16)$$

where P_{on} is the fraction of time the gene spends in the on-state, and the signal timescale is given by $\tau_\lambda = 1/(k_{\text{on}} + k_{\text{off}})$. As far as correlation coefficients are concerned, the systems of Eq. 1 and Eq. 15 behave identically and can be exactly solved analytically using the standard linear noise approach [33]. It is the Gaussian approximation for the mutual information that loses accuracy, see Fig. 4A.

While the behavior is now quantitatively different from the simple analytical approximation, the qualitative behavior remains. Reversal of Eq. 2 requires an intermediate component that is significantly faster than both X , Z , and reversal of Eq. 3 requires a cascades in which the signal timescale is longer than the lifetime of both Y , Z .

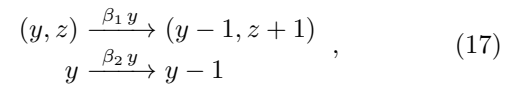
Differences between the Gaussian approximation and the exact simulation data also become apparent for the cascade define system Eq. 1 when components are present in abundances lower than two molecules on average [26].

Other types of biochemical cascades

In the previous sections we showed that mutual information can increase along the cascade defined in Eq. 1. Next, we analyze mutual information along more complex cascades to analyze the effect of molecular conversion events, or proofreading steps. (For a generalization of Eq. 1 to four components, see supplement [26].)

1. Cascades with molecular conversion events

In the cascade defined by Eq. 1 the levels of one molecule set the production rate of another. However, in biochemical cascades one molecule might convert into another through conformational changes. We first consider the case where the intermediate variable Y converts into the final read-out variable Z by replacing the production reaction of Z and the degradation reaction of Y in Eq. 1 with



where the lifetime of the intermediate component is now given by $\tau_y = 1/(\beta_1 + \beta_2)$.

Exact numerical simulations of this cascade show that Eq. 3 is now violated over a larger range of timescales, see Fig. 5A. This occurs because Z no longer inherits intrinsic noise from Y , see Appendix B. This is most easily seen in the limit where $\tau_x \gg \tau_y, \tau_z$, where the Gaussian approximation now gives

$$I(X; Z) = \frac{1}{2} \log_2 \left(1 + \frac{\eta_{\text{sig}}}{\eta_z^{\text{int}}} \right). \quad (18)$$

Compared to Eq. 13, which required $\tau_z \gg \tau_y$ for the read-out variable to remove the effect of intrinsic noise from the intermediate, in a cascade in which Y converts into Z the final read out removes the intermediate noise at all lifetimes. $I(X; Z)$ is always larger than in the case without conversions, which explains why violations occur over a wider range of timescales, see Appendix B.

In the above cascade with a final conversion event, $I(X; Z)$ decreases monotonically with τ_z . There is no advantage of time-averaging with larger τ_z when the intermediate noise is already filtered out via the conversion reaction, see Appendix B.

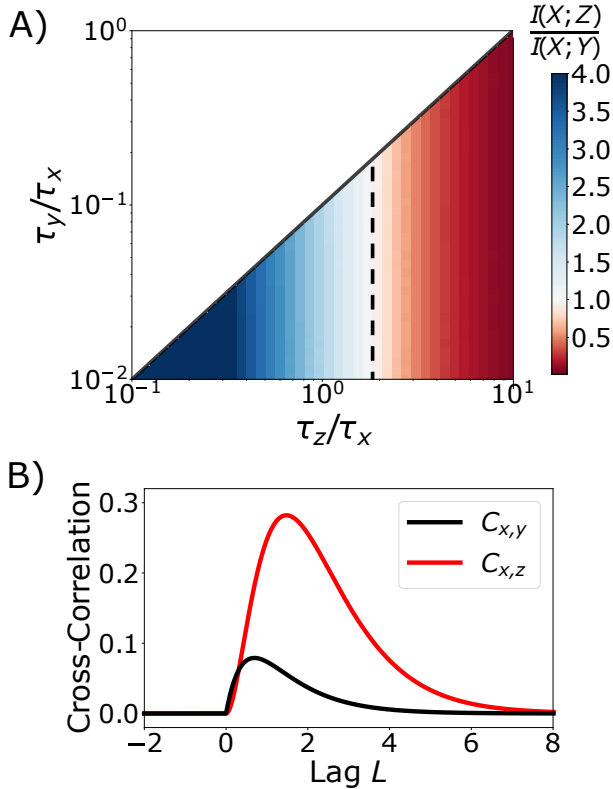
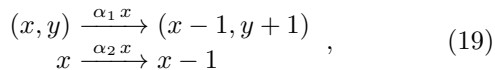


Figure 5. **Cascades with conversion events also exhibit mutual information reversal that depends on relative timescales.** A) Exact numerical simulation results for the model defined by Eq. 17 where Y -molecules are born through catalytic production and subsequently convert into Z -molecules. Data correspond to cascade with $\langle x \rangle = \langle z \rangle = 20$, and $\langle y \rangle = 2$. Cascades with conversion reactions and fixed averages are constrained in molecular lifetimes, resulting in the triangular accessible region. The (almost) vertical black dashed line corresponds to the Gaussian prediction for $I(X;Z) = I(X;Y)$ which closely matches the numerical data. B) Temporal cross-correlations between components in a linear cascade in which X converts into Y which converts into Z . Lag is measured in units of τ_x . At zero lag both cross-correlations are exactly zero because the steady state distributions are statistically independent. The causal connection between components only becomes apparent in temporal correlations with non-zero lags. Molecular abundances are the same as in panel (A) with lifetimes $\tau_x = 1, \tau_y = 0.5, \tau_z = 0.8$.

Next, we consider the cascade in which X converts into Y but Z is made catalytically. This corresponds to replacing the production reaction of Y and degradation reaction of X in Eq. 1 with



where the lifetime of the signal is now $\tau_x = 1/(\alpha_1 + \alpha_2)$.

In this cascade the stationary state distribution factorizes with $P(x, y, z) = P(x) \times P(y, z)$ where $P(x)$ is a Poisson distribution, and $P(y, z)$ is the stationary state distribution of a system in which Y is made at a constant rate reported previously [37], see Appendix B. The

initial conversion event thus makes the stationary state abundances of downstream components statistically independent of the signal and there is zero mutual information between the abundance of X and its downstream variables for any parameter values.

To illustrate why the concept of statistical independence can be dramatically misleading when applied to stationary state distributions of stochastic processes we consider the case of a conversion cascade in which both Y and Z molecules are made in conversion events. This cascade belongs to a family of reaction networks for which the stationary state distribution is the product of three independent Poisson distributions [38, 39], which implies that the mutual information between any pair of variables is strictly zero [6].

The physical dependence of these causally connected components is obscured by the statistical independence of their stationary state distributions. The interactions between biochemical components only become apparent in their temporal cross-correlation with lag L

$$C_{i,j}(L) = \frac{\langle x_i(t)x_j(t+L) \rangle - \langle x_i(t) \rangle \langle x_j(t) \rangle}{\sqrt{\text{Var}(x_i)\text{Var}(x_j)}}, \quad (20)$$

see Fig. 5B and Appendix B. This highlights how statistical concepts developed for static random variables can be highly misleading when applied to stationary state distributions of dynamically varying components in biochemical reaction networks.

When considering the stationary-state distribution, an initial conversion event will seemingly disconnect the fluctuations of the input variable from any downstream variable regardless of the length of the cascade. This can be shown by considering the general linear cascade $X_1 \rightarrow X_2 \rightarrow \dots \rightarrow X_k$, where X_1 is produced at a constant rate, and all molecules undergo first order degradation reactions while arrows denote first order production rates that can be a molecular conversion reactions or simple one component setting the production rate of the next. For all such cascades the normalized covariance between components monotonically decreases over the cascade according to

$$\frac{\text{Cov}(x_1, x_k)}{\langle x_1 \rangle \langle x_k \rangle} = \frac{\text{Cov}(x_1, x_{k-1})}{\langle x_1 \rangle \langle x_{k-1} \rangle} \frac{1}{1 + \frac{\tau_k}{\tau_1}}, \quad (21)$$

where τ_1, τ_k denote the average lifetimes of the first and k^{th} molecules in the chain. The above formula holds for $k \geq 3$, see Appendix B. Because a cascade that starts with a conversion event has $\text{Cov}(x_1, x_2) = 0$, Eq. 21 implies that all downstream covariances vanish too.

In contrast, the *rate* of mutual information transfer has been shown to be large through conversion events [6], highlighting how the mutual information of stationary state distributions cannot be used as a convenient proxy for information transfer in biochemical systems.

2. Kinetic proofreading

Finally, we consider kinetic proofreading [40, 41], which can enhance the response of cells to different ligand occupancies and is commonly argued to allow cells to better distinguish between two ligands. However, recent work has shown that the increased average differences come at the cost of increased intrinsic noise which generally worsens the ability to distinguish between different ligands [42].

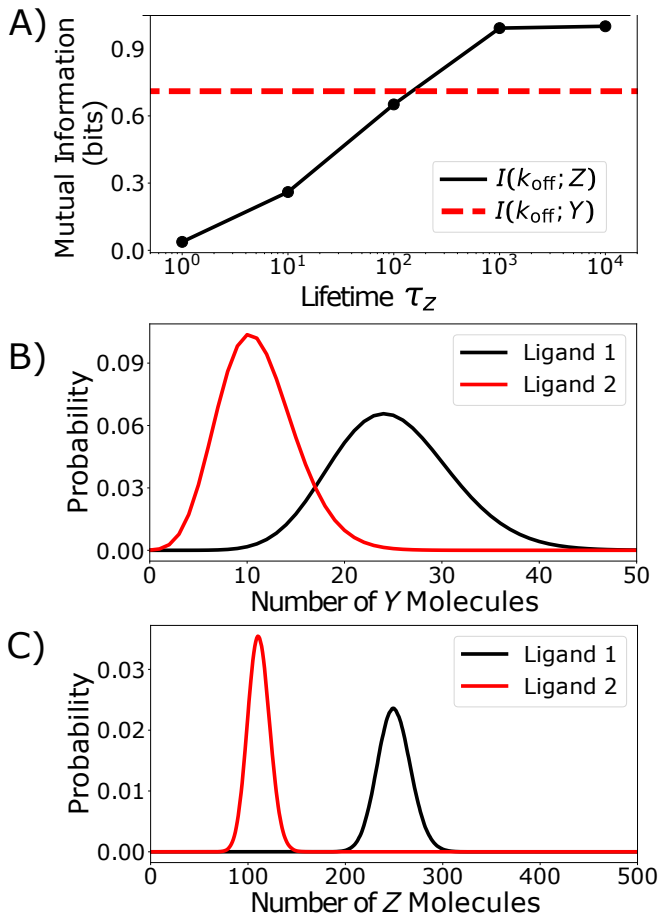


Figure 6. Time-averaging can alleviate the mutual information decreasing effect of kinetic proofreading. A) Simulation results for the kinetic proofreading model defined in the main text. Mutual information between the receptor output and the ligand dependent unbinding rate k_{off} can be increased by adding an extra component Z that time-averages the receptor output. B) The probability distribution of the receptor output. Although different ligands result in different output averages, intrinsic noise causes significant overlap of their output distributions. C) Time-averaging effectively reduces the impact of intrinsic noise in Y as illustrated by the more separated probability distribution of the final read-out variable Z .

The effect of increased intrinsic noise in kinetic proofreading has been quantified through computing mutual information between ligand affinity and receptor output [42]. We thus analyze the mutual information in the fol-

lowing model: ligands bind at a diffusion limited rate k_{on} , advance from the initial bound state to subsequent proofreading states at a rate k_f , and unbind from any state with a ligand dependent rate k_{off} . In the final bound state the receptor produces downstream signaling molecules Y at a rate k_p . The unbinding rate k_{off} depends on the ligand affinity while all other are assumed to be ligand independent. Considering two different ligands we consider the mutual information between downstream components and the unbinding rate k_{off} that takes two different values with equal probability on a timescale much slower than τ_y, τ_z .

The results of the previous sections suggest that the effect of increased intrinsic noise in proofreading can be removed through time-averaging with an additional reaction step $Y \rightarrow Z$, as long as $\tau_z \gg \tau_y$. Indeed, numerical simulation results confirm this intuition for a single receptor with two potential ligands of different affinities such that $I(k_{\text{off}}, Z)$ is larger than $I(k_{\text{off}}, Y)$, see Fig. 6A.

This result can be intuitively understood by looking at the probability distribution of output molecules. Although proofreading enhances the differences in average output associated with each ligand type, intrinsic noise can cause the resulting output distributions to overlap [42], see Fig. 6B. Adding an additional processing step with a slow read-out component can effectively reduce the impact of intrinsic noise through time-averaging, see Fig. 6C. Intrinsic noise can also be reduced by increasing the lifetime of the read-out molecule directly instead of adding an additional processing step. Both methods of increasing the mutual information come at the expense of slowing down the system response to changes in ligand concentration highlighting a general speed-accuracy trade-off in sensing systems as remarked previously [43].

DISCUSSION

The data processing inequality plays a crucial role in information theory because it sets a hard bound on the rate of information transfer between any two components that use a particular channel as an intermediary. In contrast, the mutual information between stationary state distributions of cellular abundances is not a measure of information flow [6] but a statistical measure of similarity between the distributions of molecular levels which can be increased by post-processing. In special cases it can be shown that this measure obeys strict inequalities [26], but in contrast to the fundamental data processing inequality such constraints are system specific.

Here, we clarify under which conditions the mutual information between stationary state distributions of molecular abundances behaves non-monotonically along biochemical signaling cascades. By numerically determining stationary state probability distributions of biochemical cascades we characterize the timescale dependence of the non-monotonic behavior of mutual information between molecular abundances. We complement

the exact numerical data with approximate analytical expressions by approximating the steady state distribution as multivariate Gaussian distribution similar to previous work [6, 21–23, 44]. Direct comparison with numerical simulations shows that the qualitative behavior of mutual information between components in biochemical cascades is well described by such approximations even for strongly non-Gaussian cascades.

We find that the mutual information between stationary state distributions can increase along signaling cascades with fast and noisy intermediates as long as the upstream signal is sufficiently slow. This is precisely the biologically relevant regime because for many cellular processes, the timescale of the signal is expected to be much longer than the lifetimes of the intracellular components. The mutual information between stationary state distributions of molecular abundances thus seems of limited utility for characterizing signaling processes in biology despite its convenient accessibility from experimental single-cell data.

AUTHOR CONTRIBUTIONS

RF derived the analytical results and performed the numerical simulations. RF and AH wrote the article.

DECLARATION OF INTERESTS

The authors declare that they do not have any competing interests.

ACKNOWLEDGMENTS

We thank B Kell, Seshu Iyengar, Euan Joly-Smith for many helpful discussions and suggestions. This work was supported by the Natural Sciences and Engineering Research Council of Canada and a New Researcher Award from the University of Toronto Connaught Fund.

APPENDIX

A. Two-step cascade correlations and mutual information

For chemical reaction systems with linear rates all moments can be exactly derived from the chemical master equation. In particular, the matrix of normalized (co)variances $\eta_{ij} := \text{Cov}(x_i, x_j) / (\langle x_i \rangle \langle x_j \rangle)$ satisfies the Lyapunov equation [27, 33, 45, 46]

$$M\eta + (M\eta)^T + D = 0, \quad (22)$$

where M and D for the stochastic reaction system defined by Eq. 1 are given by

$$M = \begin{pmatrix} -\frac{1}{\tau_x} & 0 & 0 \\ \frac{1}{\tau_y} & -\frac{1}{\tau_y} & 0 \\ 0 & \frac{1}{\tau_z} & -\frac{1}{\tau_z} \end{pmatrix} \quad (23)$$

$$D = \begin{pmatrix} \frac{2}{\tau_x \langle x \rangle} & 0 & 0 \\ 0 & \frac{2}{\tau_y \langle y \rangle} & 0 \\ 0 & 0 & \frac{2}{\tau_z \langle z \rangle} \end{pmatrix}.$$

Using Eqs. (22,23), one can solve for the following normalized (co)variances

$$\eta_{xx} = \frac{1}{\langle x \rangle}, \quad \eta_{xy} = \frac{1}{\langle x \rangle} \frac{1}{1 + \frac{\tau_y}{\tau_x}}$$

$$\eta_{yy} = \frac{1}{\langle y \rangle} + \frac{1}{\langle x \rangle} \frac{1}{1 + \frac{\tau_y}{\tau_x}}, \quad \eta_{xz} = \frac{1}{\langle x \rangle} \frac{1}{1 + \frac{\tau_y}{\tau_x}} \frac{1}{1 + \frac{\tau_z}{\tau_x}}$$

$$\eta_{yz} = \frac{1}{\langle y \rangle} \frac{1}{1 + \frac{\tau_z}{\tau_y}} + \frac{1}{\langle x \rangle} \frac{1}{1 + \frac{\tau_y}{\tau_x}} \left(\frac{1}{1 + \frac{\tau_z}{\tau_x}} \frac{1}{1 + \frac{\tau_y}{\tau_z}} + \frac{1}{1 + \frac{\tau_z}{\tau_y}} \right)$$

and

$$\eta_{zz} = \frac{1}{\langle z \rangle} + \eta_{yz}. \quad (24)$$

The correlation coefficients can in turn be obtained from

$$\rho_{xy} = \frac{\eta_{xy}}{\sqrt{\eta_{xx}\eta_{yy}}}, \quad (25)$$

which yields

$$\rho_{xy} = \frac{1}{1 + \frac{\tau_y}{\tau_x}} \left(\frac{1}{\frac{\langle x \rangle}{\langle y \rangle} + \frac{\tau_x}{\tau_x + \tau_y}} \right)^{1/2}$$

$$\rho_{xz} = \left[\frac{1}{1 + \frac{\tau_y}{\tau_x}} \left(\frac{1}{1 + \frac{\tau_z}{\tau_y}} + \frac{1}{1 + \frac{\tau_y}{\tau_z}} \frac{1}{1 + \frac{\tau_z}{\tau_x}} \right) + \frac{\langle x \rangle}{\langle z \rangle} + \frac{\langle x \rangle}{\langle y \rangle} \frac{1}{1 + \frac{\tau_z}{\tau_y}} \right]^{-1/2} \times \frac{1}{1 + \frac{\tau_y}{\tau_x}} \frac{1}{1 + \frac{\tau_z}{\tau_x}}$$

$$\rho_{yz} = \left[\frac{\langle x \rangle}{\langle y \rangle} \frac{1}{1 + \frac{\tau_z}{\tau_y}} + \frac{1}{1 + \frac{\tau_y}{\tau_x}} \left(\frac{1}{1 + \frac{\tau_z}{\tau_x}} \frac{1}{1 + \frac{\tau_y}{\tau_z}} + \frac{1}{1 + \frac{\tau_z}{\tau_y}} \right) \right] \times \left[\left(\frac{1}{1 + \frac{\tau_y}{\tau_x}} \left(\frac{1}{1 + \frac{\tau_z}{\tau_x}} \frac{1}{1 + \frac{\tau_y}{\tau_z}} + \frac{1}{1 + \frac{\tau_z}{\tau_y}} \right) + \frac{\langle x \rangle}{\langle z \rangle} + \frac{\langle x \rangle}{\langle y \rangle} \frac{1}{1 + \frac{\tau_z}{\tau_y}} \right) \left(\frac{\langle x \rangle}{\langle y \rangle} + \frac{1}{1 + \frac{\tau_y}{\tau_x}} \right) \right]^{-1/2}. \quad (26)$$

1. Mutual Information

Approximating the stationary state distribution of Eq. 1 as a multivariate Gaussian with the same second order moments allows us to obtain approximate analytic expressions for the mutual information via

$$I(X; Y) = -\frac{1}{2} \log_2 \left(1 - \rho_{xy}^2 \right). \quad (27)$$

The expressions obtained from applying Eq. 27 to the correlation coefficients of Eq. 26 lead to the inequalities Eq. 4 and Eq. 8 via elementary algebraic manipulations.

We find this approximation accurately describes the mutual information in our cascade unless average abundances fall below two molecules at which point the discreteness of the distribution becomes apparent [26].

To show that the lifetime ratio τ_z^*/τ_x that maximizes the mutual information $I(X; Z)$ is a decreasing function of $\eta_z^{\text{int}}/\eta_{\text{sig}}$, we note that the mutual information given by Eq. 27 is an increasing function of the correlation coefficient. When $\eta_z^{\text{int}}/\eta_{\text{sig}} \rightarrow 0$, the correlation coefficient is given by

$$\rho_{xz} = \left(\frac{1}{1 + \frac{\tau_y}{\tau_x}} \left(\frac{1}{1 + \frac{\tau_z}{\tau_y}} + \frac{1}{1 + \frac{\tau_y}{\tau_z}} \frac{1}{1 + \frac{\tau_z}{\tau_x}} \right) + \frac{\eta_y^{\text{int}}}{\eta_{\text{sig}}} \frac{1}{1 + \frac{\tau_z}{\tau_y}} \right)^{-1/2} \times \frac{1}{1 + \frac{\tau_y}{\tau_x}} \frac{1}{1 + \frac{\tau_z}{\tau_x}}. \quad (28)$$

for which a nonzero optimal time scale τ_z^* (given by Eq. 14) can exist because the denominator can decrease faster with τ_z than the numerator due to the $\eta_y^{\text{int}}/\eta_{\text{sig}}$ term.

In the regime $\eta_z^{\text{int}}/\eta_{\text{sig}} \gg \eta_y^{\text{int}}/\eta_{\text{sig}}$, 1 we have

$$\rho_{xz} = \left(\frac{\eta_{\text{sig}}}{\eta_z^{\text{int}}} \right)^{1/2} \times \frac{1}{1 + \frac{\tau_y}{\tau_x}} \frac{1}{1 + \frac{\tau_z}{\tau_x}} \quad (29)$$

for which the optimal time scale is $\tau_z^* = 0$, as the correlation coefficient is a decreasing function of τ_z . Increasing $\eta_z^{\text{int}}/\eta_{\text{sig}}$ reduces the effect of the $\eta_y^{\text{int}}/\eta_{\text{sig}}$ term monotonically, resulting in smaller optimal τ_z^* until eventually $\tau_z^* = 0$.

2. Mutual Information Inequalities

In the regime $\tau_z, \tau_y \ll \tau_x$, Eq. 4 becomes

$$1 + \frac{\tau_y}{\tau_z} \left(1 + \frac{\eta_{\text{sig}}}{\eta_y^{\text{int}}} \right) \leq \left(1 + \frac{\tau_y}{\tau_x} \right) \left(1 + \frac{\eta_{\text{sig}}}{\eta_y^{\text{int}}} \right)^{1/2}, \quad (30)$$

from which Eq. 6 follows from algebraic manipulations.

Equality of Eq. 4 implies

$$\frac{\tau_z}{\tau_x} = \frac{-\frac{\tau_y}{\tau_x} \left(1 + \frac{\eta_{\text{sig}}}{\eta_y^{\text{int}}} \left(1 + \frac{\tau_y}{\tau_x} \right) - \sqrt{\frac{\eta_{\text{sig}}}{\eta_y^{\text{int}}} + \left(1 + \frac{\tau_y}{\tau_x} \right)^{-1}} \right)}{1 + \frac{\tau_y}{\tau_x} \left(1 + \frac{\eta_{\text{sig}}}{\eta_y^{\text{int}}} \left(1 + \frac{\tau_y}{\tau_x} \right) \right) - \sqrt{\frac{\eta_{\text{sig}}}{\eta_y^{\text{int}}} + \left(1 + \frac{\tau_y}{\tau_x} \right)^{-1}}}. \quad (31)$$

When $\tau_z \gg \tau_x$, Eq. 31 implies that

$$1 + \frac{\tau_y}{\tau_x} \left(1 + \frac{\eta_{\text{sig}}}{\eta_y^{\text{int}}} \left(1 + \frac{\tau_y}{\tau_x} \right) \right) - \sqrt{\frac{\eta_{\text{sig}}}{\eta_y^{\text{int}}} + \left(1 + \frac{\tau_y}{\tau_x} \right)^{-1}} = 0. \quad (32)$$

which is a fifth order polynomial in τ_y/τ_x whose roots are analytically intractable.

However, we can obtain the roots in $\eta_{\text{sig}}/\eta_y^{\text{int}}$, given by

$$\frac{\eta_{\text{sig}}}{\eta_y^{\text{int}}} = \frac{1 - 2\frac{\tau_y}{\tau_x} - 4\frac{\tau_y^2}{\tau_x^2} - 2\frac{\tau_y^3}{\tau_x^3} \pm \sqrt{1 - 4\frac{\tau_y}{\tau_x} - \frac{\tau_y^2}{\tau_x^2}}}{2 \left(\frac{\tau_y^2}{\tau_x^2} + 2\frac{\tau_y^3}{\tau_x^3} + \frac{\tau_y^4}{\tau_x^4} \right)}. \quad (33)$$

Positivity of the variability ratios then gives rise to the necessary condition of $\tau_y/\tau_x \leq 1/2(\sqrt{2} - 1)$ to obtain equality in Eq. 4.

To obtain Eq. 9, we note the terms in Eq. 8 that are not proportional to variability measures can be grouped into a positive term on the left. Removing them yields the following necessary inequality

$$\frac{\eta_z^{\text{int}}}{\eta_{\text{sig}}} \left(1 + \frac{\tau_z}{\tau_x} \right)^2 \leq \frac{\eta_y^{\text{int}}}{\eta_{\text{sig}}} \left(1 - \frac{\left(1 + \frac{\tau_z}{\tau_x} \right)^2}{1 + \frac{\tau_z}{\tau_y}} \right). \quad (34)$$

The right side becomes larger without the term in the brackets, and algebraic manipulations then yield Eq. 9.

In the limit $\tau_z \ll \tau_x$, Eq. 8 becomes

$$1 + \frac{\tau_z}{\tau_y} \leq \frac{\eta_y^{\text{int}}}{\eta_z^{\text{int}}} \frac{\tau_z}{\tau_y} + \frac{\eta_{\text{sig}}}{\eta_z^{\text{int}}} \frac{\tau_z}{\tau_y} \frac{1}{1 + \frac{\tau_y}{\tau_x}}. \quad (35)$$

Applying the additional limit $\tau_y \ll \tau_x$ results in Eq. 10.

When $\eta_y^{\text{int}} \gg \eta_{\text{sig}}$, η_z^{int} Eq. 8 simplifies to

$$0 \leq 1 - \frac{\left(1 + \frac{\tau_z}{\tau_x} \right)^2}{1 + \frac{\tau_z}{\tau_y}}, \quad (36)$$

from which Eq. 11 follows from algebraic manipulation.

B. Cascades with conversion events

Applying Eq. 22 to the model defined in Eq. 1 and Eq. 17 yields the following normalized covariances

$$\begin{aligned}\eta_{xx} &= \frac{1}{\langle x \rangle}, & \eta_{xy} &= \frac{1}{\langle x \rangle} \frac{1}{1 + \frac{\tau_y}{\tau_x}} \\ \eta_{yy} &= \frac{1}{\langle y \rangle} + \frac{1}{\langle x \rangle} \frac{1}{1 + \frac{\tau_y}{\tau_x}}, & \eta_{xz} &= \frac{1}{\langle x \rangle} \frac{1}{1 + \frac{\tau_y}{\tau_x}} \frac{1}{1 + \frac{\tau_z}{\tau_x}} \\ \eta_{yz} &= \frac{1}{\langle x \rangle} \frac{1}{1 + \frac{\tau_y}{\tau_x}} \left(\frac{1}{1 + \frac{\tau_z}{\tau_x}} \frac{1}{1 + \frac{\tau_y}{\tau_z}} + \frac{1}{1 + \frac{\tau_z}{\tau_y}} \right) \\ \eta_{zz} &= \frac{1}{\langle z \rangle} + \frac{1}{\langle x \rangle} \frac{1}{1 + \frac{\tau_y}{\tau_x}} \left(\frac{1}{1 + \frac{\tau_z}{\tau_x}} \frac{1}{1 + \frac{\tau_y}{\tau_z}} + \frac{1}{1 + \frac{\tau_z}{\tau_y}} \right)\end{aligned}\quad (37)$$

Computing the correlation coefficients from these covariances then straightforwardly yields approximate expressions for the mutual information.

The resulting approximate $I(X; Z)$ monotonically decreases with τ_z , because Eq. 27 which is an increasing function of the correlation coefficient given by

$$\begin{aligned}\rho_{xz} &= \left(\frac{1}{1 + \frac{\tau_y}{\tau_x}} \left(\frac{1}{1 + \frac{\tau_z}{\tau_y}} + \frac{1}{1 + \frac{\tau_y}{\tau_z}} \frac{1}{1 + \frac{\tau_z}{\tau_x}} \right) + \frac{\eta_z^{\text{int}}}{\eta_{\text{sig}}} \right)^{-1/2} \\ &\times \frac{1}{1 + \frac{\tau_y}{\tau_x}} \frac{1}{1 + \frac{\tau_z}{\tau_x}}.\end{aligned}\quad (38)$$

which in turn is a decreasing function of τ_z .

For the model defined in Eq. 1 and Eq. 19, the chemical master equation is given by

$$\begin{aligned}\frac{dP(x, y, z)}{dt} &= - \left[\lambda + \frac{x}{\tau_x} + y \left(\beta + \frac{1}{\tau_y} \right) + \frac{z}{\tau_z} \right] P(x, y, z) \\ &+ \lambda P(x-1, y, z) + \alpha_2 (x+1) P(x+1, y, z) \\ &+ \alpha_1 (x+1) P(x+1, y-1, z) + \frac{y+1}{\tau_y} P(x, y+1, z) \\ &+ \beta y P(x, y, z-1) + \frac{z+1}{\tau_z} P(x, y, z+1).\end{aligned}\quad (39)$$

Substituting the ansatz $P(x, y, z) = P(x) \times P(y, z)$ into the stationary state condition of the above master equation with the Poissonian

$$P(x) = \frac{\langle x \rangle^x e^{-\langle x \rangle}}{x!}, \quad (40)$$

results in the following condition

$$\begin{aligned}0 &= - \left[\alpha_1 \langle x \rangle + y \left(\beta + \frac{1}{\tau_y} \right) + \frac{z}{\tau_z} \right] P(y, z) \\ &+ \alpha_1 \langle x \rangle P(y-1, z) + \frac{y+1}{\tau_y} P(y+1, z) \\ &+ \beta y P(y, z-1) + \frac{z+1}{\tau_z} P(y, z+1)\end{aligned}\quad (41)$$

which is satisfied as long as $P(y, z)$ is the stationary state distribution that solves the chemical master equation of a system in which Y is made at a constant rate $\alpha_1 \langle x \rangle$ and linearly affects the production of Z molecules with a rate βy . This implies that $P(x, y, z) = P(x) \times P(y, z)$ is indeed the stationary state distribution of the model defined in Eq. 1 and Eq. 19 as claimed in the main text.

The cross-correlations of the conversion cascade in which both Y and Z molecules are made in conversion events can be derived from the corresponding chemical master equation [47]. For $L < 0$ the temporal cross-correlations are zero and for $L \geq 0$ we obtain

$$\begin{aligned}C_{x,y}(L) &= \sqrt{\frac{\eta_{\text{sig}}}{\eta_y^{\text{int}}}} \frac{e^{-L/\tau_y} - e^{-L/\tau_x}}{1 - \frac{\tau_x}{\tau_y}} \\ C_{x,z}(L) &= \frac{1}{\tau_x \tau_y} \sqrt{\frac{\eta_{\text{sig}}}{\eta_z^{\text{int}}}} \left(\left(\frac{1}{\tau_x} - \frac{1}{\tau_y} \right) \left(\frac{1}{\tau_x} - \frac{1}{\tau_z} \right) \left(\frac{1}{\tau_y} - \frac{1}{\tau_z} \right) \right)^{-1} \\ &\times \left(e^{-L/\tau_z} \left(\frac{1}{\tau_x} - \frac{1}{\tau_y} \right) + e^{-L/\tau_x} \left(\frac{1}{\tau_y} - \frac{1}{\tau_z} \right) \right. \\ &\left. + e^{-L/\tau_y} \left(\frac{1}{\tau_z} - \frac{1}{\tau_x} \right) \right),\end{aligned}\quad (42)$$

which are plotted in the main text.

To derive Eq. 21, we utilize the fluctuation balance equations that must be satisfied by any pairs of components X_i and X_j in a system with stationary probability distributions [46]

$$\text{Cov}(x_i, R_j^- - R_j^+) + \text{Cov}(x_j, R_i^- - R_i^+) = \sum_{k=1}^N s_{ki} s_{kj} \langle r_k \rangle, \quad (43)$$

where x_i is the abundance of molecule X_i , R_j^\pm is the total flux of production or degradation for molecule X_j , and $\langle r_k \rangle$ is the average reaction rate for reaction k in which levels of X_i are changed by s_{ki} .

For the linear cascade $X_1 \rightarrow X_2 \rightarrow \dots \rightarrow X_k$, Eq. 43 yields the following relation for $k > 2$

$$\text{Cov}(x_1, -R_k) + \text{Cov}(x_k, -R_1) = 0, \quad (44)$$

with reaction fluxes are given by

$$R_1 = \lambda - \frac{x_1}{\tau_1}, R_k = c_k x_{k-1} - \frac{x_k}{\tau_k}, \quad (45)$$

where λ is the production rate of the first molecule, $c_k x_{k-1}$ is the rate at which molecule X_{k-1} converts into molecule X_k , and τ_k the lifetime of the k^{th} molecule. Algebraic manipulations then result in Eq. 21.

-
- [1] C. E. Shannon, *The Bell System Technical Journal* **27**, 379 (1948).
- [2] J. O. Dubuis, G. Tkačik, E. F. Wieschaus, T. Gregor, and W. Bialek, *Proceedings of the National Academy of Sciences* **110**, 16301 (2013).
- [3] I. Lestas, G. Vinnicombe, and J. Paulsson, *Nature* **467**, 174 (2010).
- [4] A.-L. Moor and C. Zechner, *Phys. Rev. Res.* **5**, 013032 (2023).
- [5] F. Tostevin and P. R. Ten Wolde, *Physical Review Letters* **102**, 218101 (2009).
- [6] F. Tostevin and P. R. Ten Wolde, *Physical Review E* **81**, 061917 (2010).
- [7] W. H. de Ronde, F. Tostevin, and P. R. Ten Wolde, *Physical Review E* **82**, 031914 (2010).
- [8] H. H. Mattingly, K. Kamino, B. B. Machta, and T. Emonet, *Nature physics* **17**, 1426 (2021).
- [9] T. M. Cover and J. A. Thomas, *Elements of Information Theory (Wiley Series in Telecommunications and Signal Processing)* (Wiley-Interscience, USA, 2006).
- [10] M. Meijers, S. Ito, and P. R. Ten Wolde, *Physical Review E* **103**, L010102 (2021).
- [11] L. Duso and C. Zechner, in *2019 IEEE 58th Conference on Decision and Control (CDC)* (IEEE, 2019) pp. 6610–6615.
- [12] M. Reinhardt, G. Tkačik, and P. R. Ten Wolde, *Physical Review X* **13**, 041017 (2023).
- [13] Y. Taniguchi, P. J. Choi, G.-W. Li, H. Chen, M. Babu, J. Hearn, A. Emili, and X. S. Xie, *Science* **329**, 533 (2010).
- [14] C. Vogel and E. M. Marcotte, *Nature Reviews Genetics* **13**, 227 (2012).
- [15] L. F. Vistain and S. Tay, *Trends in Biochemical Sciences* **46**, 661 (2021).
- [16] B. Munsky, G. Neuert, and A. van Oudenaarden, *Science* **336**, 183 (2012).
- [17] A. Hilfinger and J. Paulsson, *Proc. Natl. Acad. Sci. U. S. A.* **108**, 12167 (2011).
- [18] C. G. Bowsher and P. S. Swain, *Proceedings of the National Academy of Sciences* **109**, E1320 (2012).
- [19] C. G. Bowsher, M. Voliotis, and P. S. Swain, *PLoS computational biology* **9**, e1002965 (2013).
- [20] E. Ziv, I. Nemenman, and C. H. Wiggins, *PloS One* **2**, e1077 (2007).
- [21] A. Biswas and S. K. Banik, *Physical Review E* **93**, 052422 (2016).
- [22] M. Nandi, S. K. Banik, and P. Chaudhury, *Physical Review E* **100**, 032406 (2019).
- [23] T. S. Roy, M. Nandi, A. Biswas, P. Chaudhury, and S. K. Banik, *Theory in Biosciences* **140**, 295 (2021).
- [24] K. R. Pilikiewicz and M. L. Mayo, *Physical Review E* **94**, 032412 (2016).
- [25] M. A. Rowland, K. R. Pilikiewicz, and M. L. Mayo, *PLoS One* **16**, e0245094 (2021).
- [26] See supplemental material at [url will be inserted].
- [27] J. Paulsson, *Phys. Life Rev.* **2**, 157 (2005).
- [28] A. Borst and F. E. Theunissen, *Nature Neuroscience* **2**, 947 (1999).
- [29] F. Tostevin and P. R. Ten Wolde, *Physical Review E* **81**, 061917 (2010).
- [30] W. De Ronde, F. Tostevin, and P. R. ten Wolde, *Physical Review E* **86**, 021913 (2012).
- [31] F. Mancini, C. H. Wiggins, M. Marsili, and A. M. Walczak, *Physical Review E* **88**, 022708 (2013).
- [32] D. T. Gillespie, *J. Phys. Chem.* **81**, 2340 (1977).
- [33] J. Paulsson, *Nature* **427**, 415 (2004).
- [34] T. Gedeon and P. Bokes, *Biophys. J.* **103**, 377 (2012).
- [35] H. C. Berg and E. M. Purcell, *Biophysical Journal* **20**, 193 (1977).
- [36] S. Haykin and B. Van Veen, *Signals and systems* (John Wiley & Sons, 2007).
- [37] Y. Li, D.-Q. Jiang, and C. Jia, *Physical Review E* **104**, 024408 (2021).
- [38] D. F. Anderson, G. Craciun, and T. G. Kurtz, *Bulletin of mathematical biology* **72**, 1947 (2010).
- [39] J. C. Baez and J. Biamonte, *Quantum techniques for stochastic mechanics*, arXiv:1209.3632v5 (2019), [quant-ph].
- [40] J. J. Hopfield, *Proceedings of the National Academy of Sciences* **71**, 4135 (1974).
- [41] J. Ninio, *Biochimie* **57**, 587 (1975).
- [42] D. Kirby and A. Zilman, *Proceedings of the National Academy of Sciences* **120**, e2212795120 (2023).
- [43] G. Lan, P. Sartori, S. Neumann, V. Sourjik, and Y. Tu, *Nature Physics* **8**, 422 (2012).
- [44] M. Nandi, A. Biswas, S. K. Banik, and P. Chaudhury, *Physical Review E* **98**, 042310 (2018).
- [45] N. G. Van Kampen, *Stochastic processes in physics and chemistry* (Elsevier, 1992).
- [46] A. Hilfinger, T. M. Norman, G. Vinnicombe, and J. Paulsson, *Phys. Rev. Lett.* **116**, 058101 (2016).
- [47] W. J. Heuett and H. Qian, *The Journal of Chemical Physics* **124**, 044110 (2006).

Characterizing the non-monotonic behavior of mutual information along biochemical reaction cascades: Supplemental Material

Raymond Fan and Andreas Hilfinger

andreas.hilfinger@utoronto.ca

In this document we present the results of numerical simulations of the system defined by Eq. 1 for abundances different than those reported in Fig. 1 and Fig. 3. Furthermore, we present the corresponding analysis of longer cascades with four components, and derive an example bound that constrains the mutual information between stationary state distributions in a simple cascade.

Numerical simulations of of Eq. 1 For Different Abundances

We simulate the model defined by Eq. 1 for several average abundances. First, we explore the effect of different Z abundances compared to the main text.

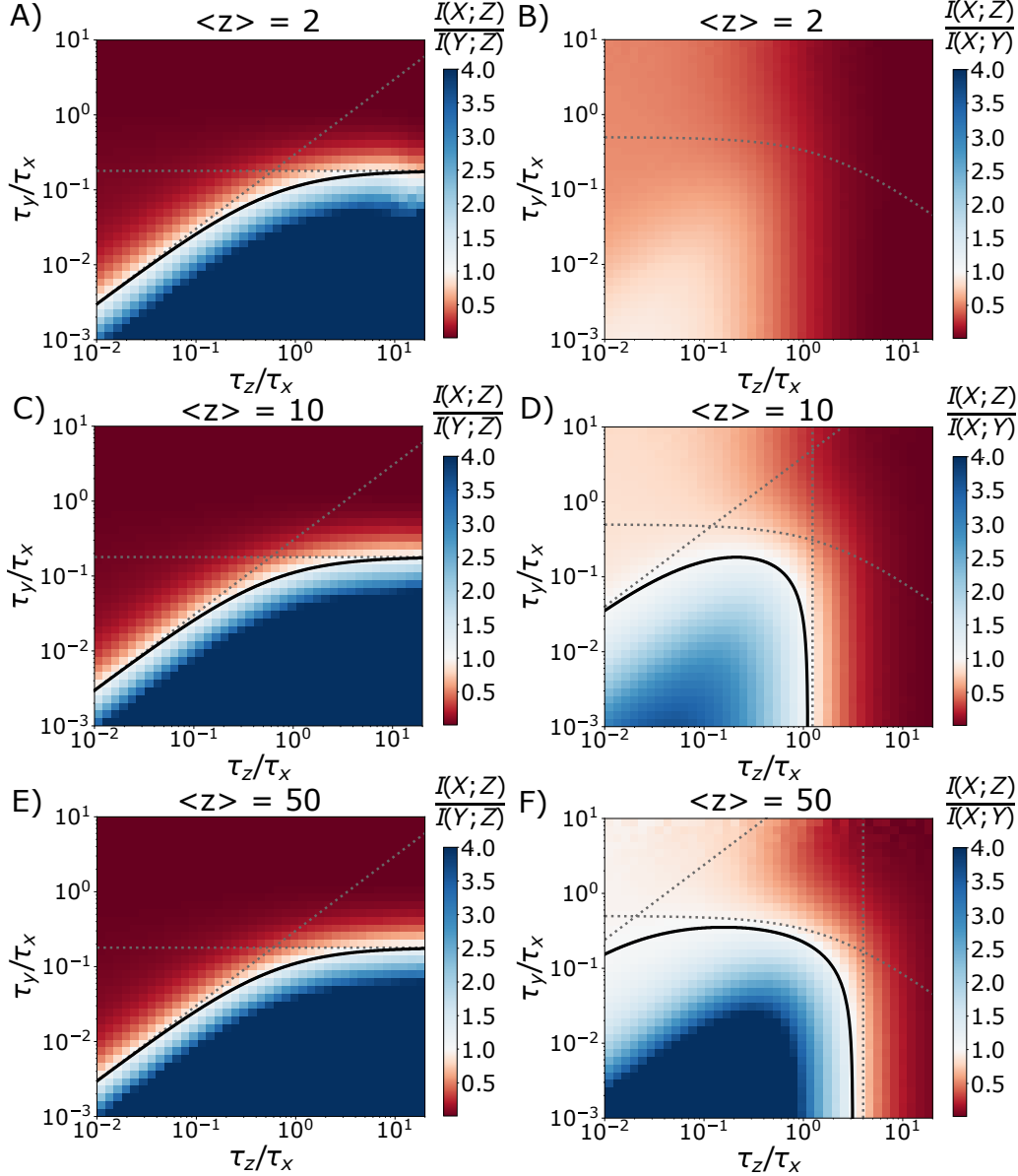


Figure S1: **Simulating Eq. 1 for different Z abundances.** We plot exact numerical simulation results for the mutual information between pairs of variables in the cascade defined by Eq. 1. Blue region indicates the parameter regime in which Eq. 2 and Eq. 3 of the main text are violated. Plots are generated for $\langle x \rangle = 20$, $\langle y \rangle = 2$ and varying $\langle z \rangle$. A) C) E) correspond to $I(X;Z)/I(Y;Z)$, where the solid black line corresponds to Eq. 4 of the main text, and the dashed gray lines correspond to the simpler inequalities derived in the main text. There is little dependence on $\langle z \rangle$ here. B) D) F) correspond to $I(X;Z)/I(X;Y)$, where the solid black line corresponds to Eq. 8 of the main text, and the dashed gray lines correspond to the simpler inequalities of Eqs. 9–11 in the main text.

Next, we analyze the effect of varying all averages by a constant scale factor U .

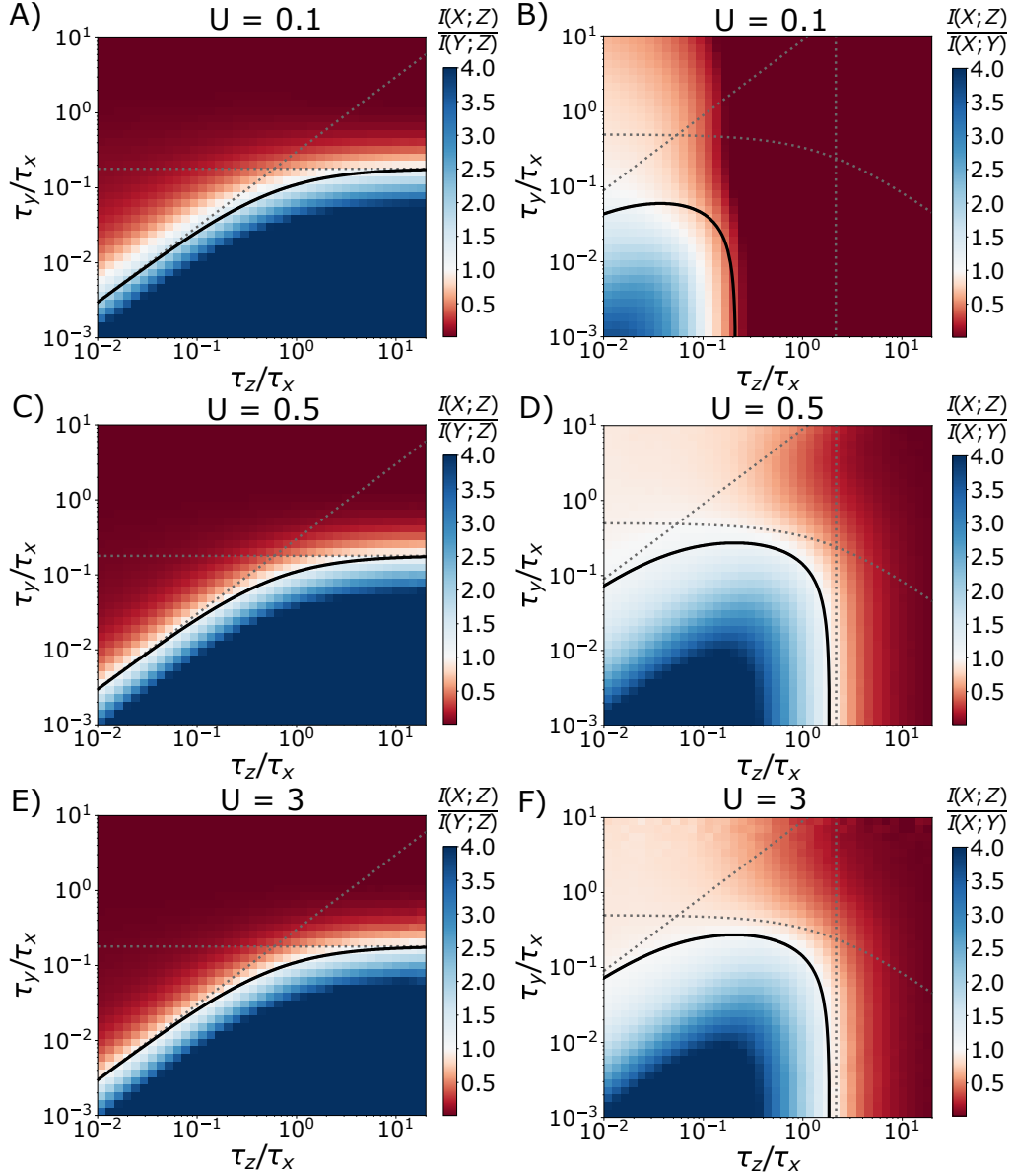


Figure S2: **Simulating Eq. 1 for different abundance scales.** We plot exact numerical simulation results for the mutual information between pairs of variables in the cascade defined by Eq. 1. Blue region indicates the parameter regime in which Eq. 2 and Eq. 3 of the main text are violated. Plots are generated for $\langle x \rangle = \langle z \rangle = 20U$, $\langle y \rangle = 2U$, where U is a scaling factor. A) C) E) correspond to $I(X;Z)/I(Y;Z)$, where the solid black line corresponds to Eq. 4 of the main text, and the dashed gray lines correspond to the simpler inequalities derived in the main text. We observe only a minor dependence on the behavior on the overall scale U . B) D) F) correspond to $I(X;Z)/I(X;Y)$, where the solid black line corresponds to Eq. 8 of the main text, and the dashed gray lines correspond to the simpler inequalities Eq. 9–11 in the main text.

Finally, following our results for the stochastic switch model of Eq. 15, we simulate Eq. 1 with $\langle x \rangle = 0.5$, obtaining similar results to the plots of Fig. 4.

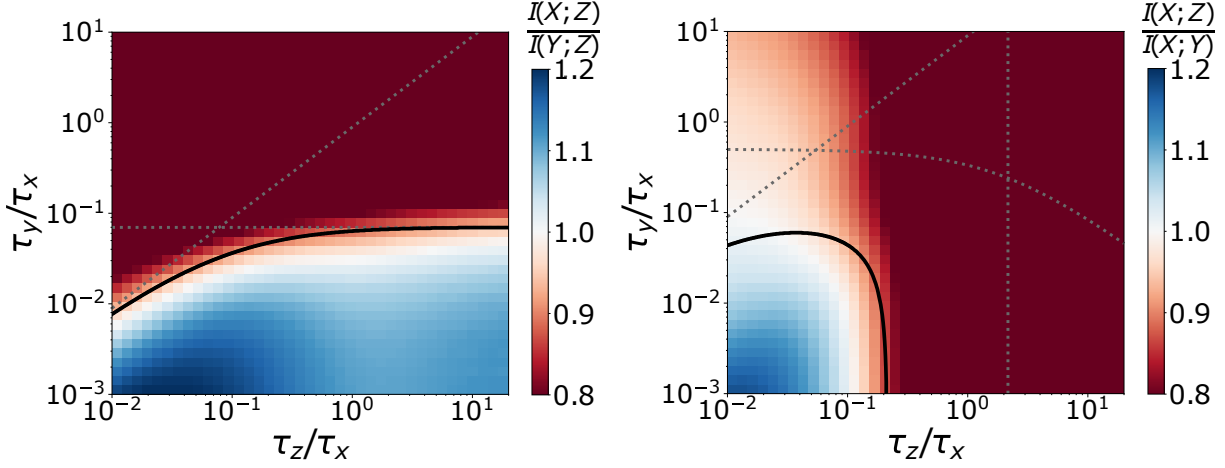


Figure S3: **On-off upstream signals and Poissonian signals with low X averages behave similarly. In both cases the Gaussian approximations make accurate qualitative but not quantitative predictions.** B) Exact numerical simulations of the system defined by Eq. 1 in the main text for $\langle x \rangle = 0.5, \langle y \rangle = 2, \langle z \rangle = 20$. The Gaussian approximation (black line) no longer quantitatively predicts the region of violations, but qualitative time-scale features are accurately characterized, i.e., Eq. 2 is not obeyed when the intermediate Y is significantly faster than both X, Z , and Eq. 3 is not obeyed when the signal timescales are longer lived than all other components. This is similar to the results obtained for the on-off upstream signal defined in the Eq. 15 of the main text and plotted in Fig. 4B.

Three step cascades

Arguably, the analysis of the two-step cascade of Eq. 1 corresponds to a special case in which all tested inequalities involved the mutual information between a Poisson variable and a downstream component. We thus next analyze the mutual information between the second, third, and fourth component in a three-step cascade. We consider the dynamics of Eq. 1 with the following additional reactions



Numerical simulations show that it is again possible for mutual information to be larger between more distant variables. The parameters for this regime are similar to the original two step cascade, where the intrinsic noise of the intermediate (now Z), and the lifetimes of downstream components must be small compared to the timescale of the upstream variability.

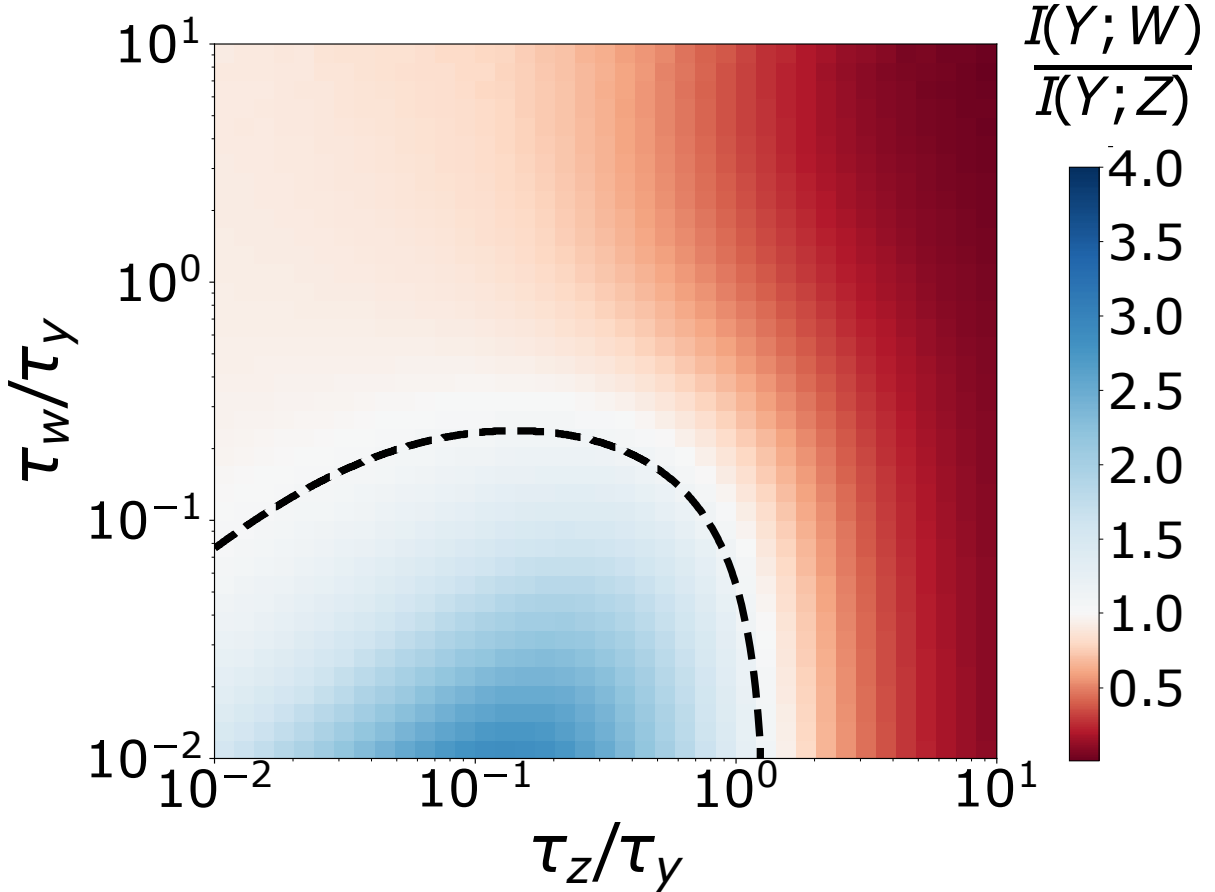


Figure S4: **Non-monotonic behavior of mutual information in longer linear cascades.** Exact numerical simulation results for the ratio of mutual information $I(Y;W)/I(Y;Z)$ for the model defined in Eq. 1 of the main text and Eq. S.1 of the supplement, reveals that $I(Y;W) > I(Y;Z)$ can occur. This shows that mutual information can increase along a cascade even when the upstream signal is no longer a Poissonian variable. The graph was generated for $\langle x \rangle = 0.5, \langle y \rangle = \langle w \rangle = 20, \langle z \rangle = 2, \tau_x = 0.1, \tau_y = 1$.

This cascade also allows us to study the behavior of mutual information over multiple intermediates, for which it has been previously shown that the mutual information can increase for certain parameters (Refs. [23, 24] of the main text). Our analytical approximation suggests such violations occur because Eq. 13 generalizes to longer, meaning the noise of multiple intermediates can be eliminated depending on the relative lifetimes of the molecules involved.

The covariances in the three step cascade are given by Eq. 25 along with the following additional covariances

$$\begin{aligned}
\eta_{xw} &= \frac{1}{\langle x \rangle} \frac{1}{1 + \frac{t_y}{t_x}} \frac{1}{1 + \frac{t_z}{t_x}} \frac{1}{1 + \frac{\tau_w}{\tau_x}} \\
\eta_{yw} &= \frac{1}{\langle x \rangle} \frac{1}{1 + \frac{\tau_y}{\tau_x}} \left(\frac{1}{1 + \frac{\tau_w}{\tau_y}} \left(\frac{1}{1 + \frac{\tau_z}{\tau_x}} \frac{1}{1 + \frac{\tau_y}{\tau_z}} + \frac{1}{1 + \frac{\tau_z}{\tau_y}} \right) + \frac{1}{1 + \frac{\tau_y}{\tau_w}} \frac{1}{1 + \frac{t_z}{t_x}} \frac{1}{1 + \frac{\tau_w}{\tau_x}} \right) + \frac{1}{\langle y \rangle} \frac{1}{1 + \frac{t_z}{t_y}} \frac{1}{1 + \frac{\tau_w}{\tau_y}} \\
\eta_{zw} &= \frac{1}{\langle x \rangle} \frac{1}{1 + \frac{\tau_y}{\tau_x}} \left(\frac{1}{1 + \frac{\tau_w}{\tau_y}} \left(\frac{1}{1 + \frac{\tau_z}{\tau_x}} \frac{1}{1 + \frac{\tau_y}{\tau_z}} + \frac{1}{1 + \frac{\tau_z}{\tau_y}} \right) + \frac{1}{1 + \frac{\tau_z}{\tau_w}} \frac{1}{1 + \frac{\tau_w}{\tau_y}} \left(\frac{1}{1 + \frac{\tau_z}{\tau_x}} \frac{1}{1 + \frac{\tau_y}{\tau_z}} + \frac{1}{1 + \frac{\tau_z}{\tau_y}} \right) \right) \\
&\quad + \frac{1}{1 + \frac{\tau_y}{\tau_w}} \frac{1}{1 + \frac{\tau_z}{\tau_x}} \frac{1}{1 + \frac{\tau_w}{\tau_x}} \Big) + \frac{1}{\langle z \rangle} \frac{1}{1 + \frac{\tau_w}{\tau_z}} + \frac{1}{\langle y \rangle} \frac{1}{1 + \frac{\tau_z}{\tau_y}} \left(\frac{1}{1 + \frac{\tau_w}{\tau_z}} + \frac{1}{1 + \frac{\tau_w}{\tau_y}} \frac{1}{1 + \frac{\tau_z}{\tau_w}} \right) \\
\eta_{ww} &= \frac{1}{\langle w \rangle} + \eta_{zw} \quad .
\end{aligned} \tag{S.2}$$

from which approximate expressions for the mutual information can be derived via the Gaussian approximation.

Bounds on mutual information between stationary state distributions

In this section, we derive and analyze a tight bound for the mutual information in the steady state distributions of all reaction networks with an on-off upstream connected via a linear production rate to arbitrarily complex downstream components, which is a generalization of the system defined in Eq. 15 of the main text.

A trivial bound on all mutual information is the entropy

$$I(X; Y) \leq H(X), H(Y) \tag{S.3}$$

which follows from the definition of mutual information, and does not depend on the details of the system like the data-processing inequality. Violations imply an error in calculating these quantities from the corresponding joint probability distribution, and are not helpful in analyzing biochemical systems.

Tighter bounds can be derived by specifying details of the system. When an upstream component X is connected to downstream components through a linear production rate as follows



then the mutual information between X and an arbitrary downstream component Z that depends on X only through Y as an intermediary is bound by

$$I(X; Z) \leq I(X; \vec{T} = (t_1, t_2, t_3 \dots)) \tag{S.5}$$

where \vec{T} is an infinite dimensional vector that contains the times at which every Y birth event is observed. This follows by definition as Z can only obtain information about X from the Y birth events. For example, in the process defined by Eq. 1, Z was a form of time-averaging of Y , where it effectively counts the more recent Y birth events. However, time-averaging is one of many methods to construct a downstream variable Z , and does not necessarily maximize the mutual information.

While Eq. S.5 is true for all networks with the reaction Eq. S.4, the distribution $P(X, \vec{T})$ is experimentally inaccessible because it requires measuring an infinite number of Y birth events. A finite number of event times can be obtained in a simulation with specified X dynamics, but it is unclear how accurate finite representations of $P(X, T_{event})$ will affect the mutual information.

The problem of infinite dimensional distributions are avoided when considering an on-off signal of the form



for which the state of the upstream is known exactly when a birth event is observed. This form of signal was considered in Eq. 15 of the main text. For this signal, a birth event at $t = t_0$ implies $x(t_0) = x_{\text{on}}$, and there is no additional information on the future values of X gained by knowing the history of x beyond knowing the current value of X . This implies all information about the current value of x is contained only in the time of most recent birth event, and thus $I(x; \vec{T}) = I(X; T_{\text{last event}})$. The probability distribution $P(X, T_{\text{last event}})$ can be obtained from a Gillespie simulation, or directly from the chemical master equation.

Note it is not sufficient for only the current value of X to be known exactly. Even a signal X that can only take on two values can in general depend on a larger network. The history of X can thus contain information about the state of this larger network, and $I(x; \vec{T}) \neq I(x; T_{\text{last event}})$. For example, if X is periodically driven, then past values of X can be used to infer the period and phase.

Proceeding with the analysis of the signal defined by Eq. S.6, yields the following upper bound

$$\begin{aligned} I(X; Z) \leq & H(P_{\text{on}}) + \frac{NP_{\text{on}}}{\sqrt{(N + \frac{1}{P_{\text{off}}})^2 - 4N\frac{P_{\text{on}}}{P_{\text{off}}}}} \times \int_0^\infty \left[(e^{r_2 t} - e^{r_1 t}) \log(e^{r_2 t} - e^{r_1 t}) \right. \\ & + \left(\left(\frac{P_{\text{on}}}{P_{\text{off}}} + r_2 \right) e^{r_2 t} - \left(\frac{P_{\text{on}}}{P_{\text{off}}} + r_1 \right) e^{r_1 t} \right) \times \log \left(\left(\frac{P_{\text{on}}}{P_{\text{off}}} + r_2 \right) e^{r_2 t} - \left(\frac{P_{\text{on}}}{P_{\text{off}}} + r_1 \right) e^{r_1 t} \right) \\ & \left. - \left(\left(\frac{1}{P_{\text{off}}} + r_2 \right) e^{r_2 t} - \left(\frac{1}{P_{\text{off}}} + r_1 \right) e^{r_1 t} \right) \times \log \left(\left(\frac{1}{P_{\text{off}}} + r_2 \right) e^{r_2 t} - \left(\frac{1}{P_{\text{off}}} + r_1 \right) e^{r_1 t} \right) \right] dt \end{aligned} \quad (\text{S.7})$$

where P_{on} is the fraction of the time x spends in the on state, N is the average number of birth events that occur during one instance of the on state, $H(X)$ is the binary entropy function and r_2, r_1 are given by

$$r_{2,1} = \frac{1}{2} \left(-N - \frac{1}{P_{\text{off}}} \pm \sqrt{\left(N + \frac{1}{P_{\text{off}}} \right)^2 - 4N\frac{P_{\text{on}}}{P_{\text{off}}}} \right) \quad (\text{S.8})$$

The right-hand-side of Eq. S.7 cannot be solved analytically but it can be evaluated numerically as a function of P_{on} and N , see Fig. S5.

Intuitively, mutual information is an increasing function of N . A large rate of events implies that when events have not been observed for a long time (relative to characteristic timescale τ_x) then the upstream must be in the off state. Conversely, a low event frequency N makes it difficult to infer the current value of x . This intuition agrees with our solution as shown by Fig. S5. Furthermore, for $N = 10000$ it can be shown that $I(x; z) \approx H(P_{\text{on}})$, see Appendix .

The behavior at intermediate N is more complicated. Although $I(X; Z)$ for very small and large N are symmetric in P_{on} , at intermediate values an asymmetry occurs where mutual information $I(X; Z)$ is larger for $P_{\text{on}} \leq 0.5$ than for $P_{\text{on}} \geq 0.5$. As a result, although the maximum entropy occurs at $H(P_{\text{on}} = 0.5)$, the maximum mutual information for intermediate N occurs at a lower value of P_{on} .

Since $N = \langle y \rangle \tau_y / \langle x \rangle \tau_x$ when Y undergoes first order degradation, this bound can be directly applied to our previous results for the process defined in Eq. 15 of the main text, which had the same form of upstream signal as the model solved here. This comparison reveals that time-averaging performs fairly comparable to the theoretical limit for large N , but that there exist better methods of generating a Z with high mutual information for low N .

Although the bound of Eq. S.7 can be formulated in terms of experimentally measurable variables such as averages and lifetimes, it only applies to a specific linear cascade with an on-off input signal unlike the data-processing inequality which holds for all Markov Chains without any assumptions about their specific dependencies and input signals.

Furthermore, the utility of the data-processing inequality is also not limited to computing

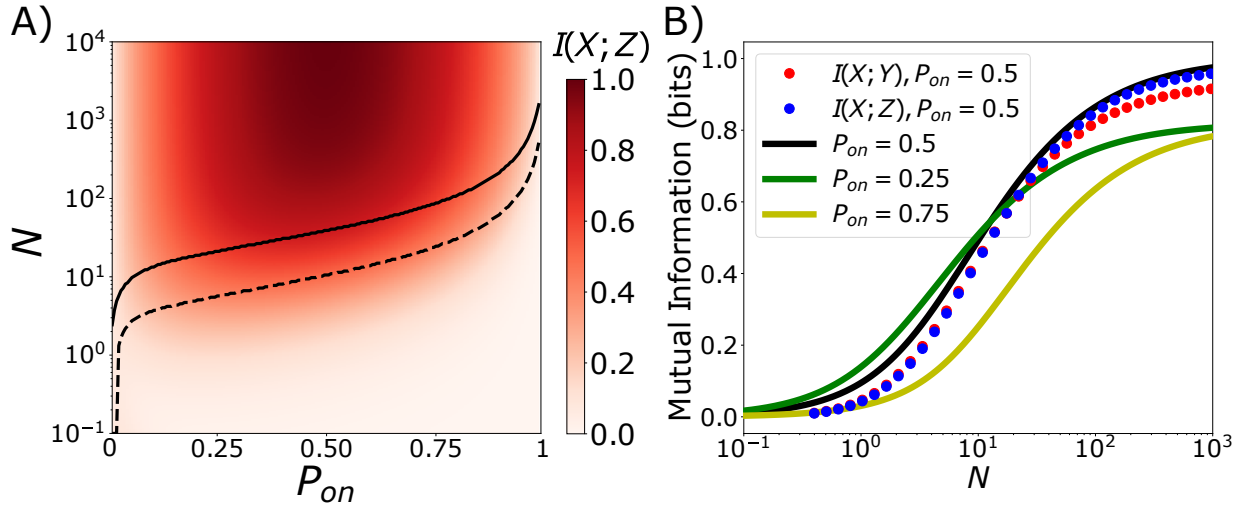


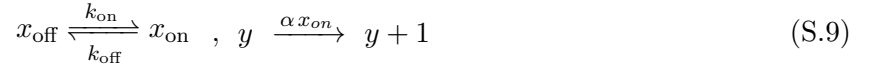
Figure S5: **The maximum mutual information between a stochastic on-off signal X and any downstream variable Z depends on probability of the signal to be in its on-state P_{on} and the average number of Y molecules produced during the on-state of the signal, N .** A) For the upstream signal defined by Eq. S.6, the maximum mutual information between the steady state distributions of Z and any downstream variable Z that depends on X only through birth events of an intermediate molecule Y that occur at rate αx is given by Eq. S.7. Although this integral cannot be solved analytically, it can be plotted as a function of $\langle x \rangle = P_{\text{on}}$ and N . This plot shows that the mutual information rises with N as expected, since more events provide more information for Z . The solid black line indicates where $I(X; Z) = 0.5 \times H(P_{\text{on}})$ while the dashed line indicates $I(X; Z) = 0.25 \times H(P_{\text{on}})$. $H(P_{\text{on}})$ is the binary entropy function, which is the maximum possible mutual information for this system. There is an asymmetry where smaller P_{on} result in larger potential mutual information. B) Plotting the maximum mutual information $I(X; Z)$ as a function of N for several values of P_{on} (colored lines) reveals that the mutual information rapidly increases for $N \geq 10$. We compare our theoretical prediction to results from simulating Eq. S.6 for $P_{\text{on}} = 0.5$ (dots), and we find the maximum mutual information achieved by time-averaging in our two step cascade is close to the theoretical limit when $N > 10$, but performs significantly worse when N is small.

bounds and ruling out particular network motifs. Bounding the mutual information across any network which uses a particular channel as an intermediary motivates the study of small network motifs as they yield an upper limit on larger networks. Meanwhile the approach outlined here only finds bounds on the mutual information between a specified signal and the variables downstream and does not apply if the signal of interest lies further upstream.

Finally, note that the mutual information limited by the data-processing inequality is the information transferred across the network, which is easy to interpret and has clear relevance to biological systems. The mutual information between stationary state distributions considered here is less clear, as the steady state distributions are generated through sampling the actual temporal process through which communication occurs.

Derivation of Eq. S.7

For the following model



we derive the probability distribution $P(X, T_{\text{last event}})$. This is the probability of a particular X state and time since the last event $t = T_{\text{last event}}$, and obeys the following ODEs

$$\begin{aligned} \frac{dP(x_{\text{on}}, t)}{dt} &= -(\alpha + k_{\text{off}})P(x_{\text{on}}, t) + k_{\text{on}}P(x_{\text{off}}, t) \\ \frac{dP(x_{\text{off}}, t)}{dt} &= -k_{\text{on}}P(x_{\text{off}}, t) + k_{\text{off}}P(x_{\text{on}}, t) \end{aligned} \quad (\text{S.10})$$

where the two X states flip between each other with rates $k_{\text{on}}, k_{\text{off}}$, and the total probability decreases through the x_{on} state due to the possibility of a new birth event. The general solution is

$$P(1, t) = c_1 \frac{k_{\text{on}} + r_1}{k_{\text{off}}} e^{r_1 t} + c_2 \frac{k_{\text{on}} + r_2}{k_{\text{off}}} e^{r_2 t} \quad (\text{S.11})$$

$$P(0, t) = c_1 e^{r_1 t} + c_2 e^{r_2 t} \quad (\text{S.12})$$

where c_1, c_2 are undetermined constants, and the eigenvalues are

$$r_{1,2} = \frac{-\alpha - k_{\text{off}} - k_{\text{on}} \pm \sqrt{\alpha^2 + 2(k_{\text{off}} + k_{\text{on}})\alpha + k_{\text{off}}^2 + 2k_{\text{on}}k_{\text{off}} + k_{\text{on}}^2}}{2} \quad (\text{S.13})$$

Note that for our system $P(0, t) = 0$ birth events can only occur if X is in its on-state and thus $c_1 = -c_2$. Furthermore, the total probability of all possible X states and times must sum to zero, which implies

$$1 = \int_0^\infty (P(0, t) + P(1, t)) dt = c_1 \left(\frac{k_{\text{on}} + k_{\text{off}}}{r_1 r_2} \right). \quad (\text{S.14})$$

This yields the following probability distribution

$$\begin{aligned} P(1, t) &= k_{\text{on}} \frac{e^{r_2 t} - e^{r_1 t}}{r_2 - r_1} + \frac{r_2 e^{r_2 t} - r_1 e^{r_1 t}}{r_2 - r_1} \\ P(0, t) &= k_{\text{off}} \frac{e^{r_2 t} - e^{r_1 t}}{r_2 - r_1} \end{aligned} \quad (\text{S.15})$$

which is plotted in Fig. S6A.

The mutual information can be computed from $I(X;Y) = H(X) + H(Y) - H(X;Y)$, where marginal and joint entropies are given by

$$H(X) = P_{on} \log_2(P_{on}) \quad (\text{S.16})$$

$$H(T_{\text{last event}}) = \int_0^\infty P(t) \log(P(t)) dt \quad (\text{S.17})$$

$$H(X, T_{\text{last event}}) = \int_0^\infty P(0,t) \log\left(\frac{P(0,t)}{P(0)P(t)}\right) + P(1,t) \log\left(\frac{P(1,t)}{P(1)P(t)}\right) dt \quad (\text{S.18})$$

resulting in Eq. S.7. Although there is no closed form solution to this integral, one can plot it numerically as shown in Fig. S6B.

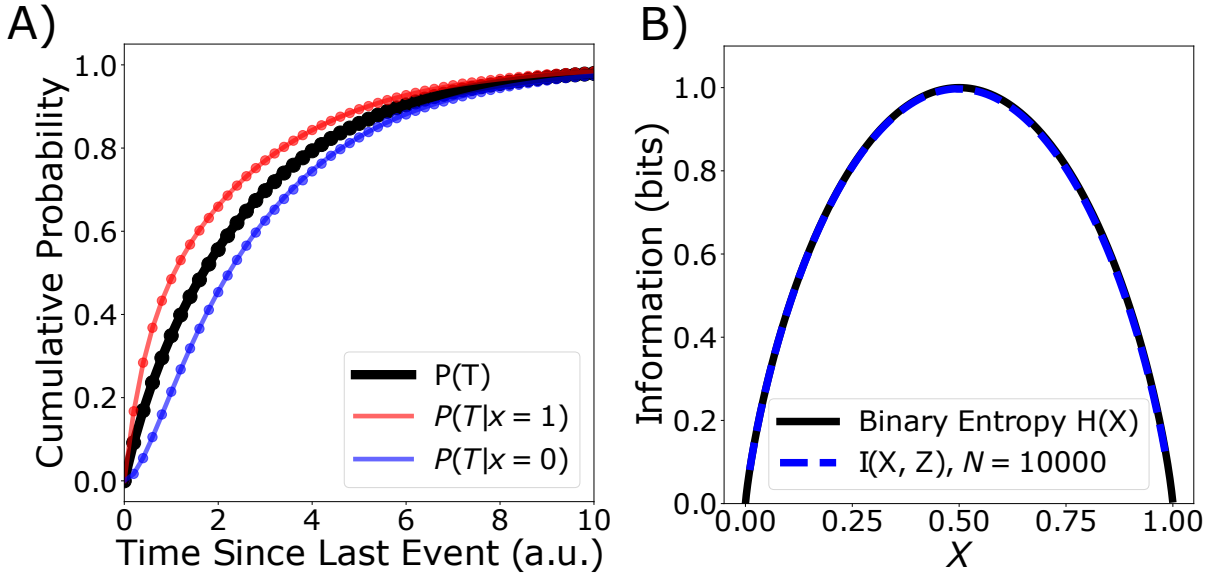


Figure S6: **Comparing analytical results from solving the model defined by Eq. S.9 with numerical predictions for $P(T|x)$ and $H(X)$.** A) To verify the probability distribution of Eq. S.15, we ran a Gillespie simulation for Eq. S.9 and sampled the system at random times to obtain the distribution $P(X, T_{\text{last event}})$. Comparing this distribution (dots) with our analytical results (line) reveals a good agreement between the theory and simulation. Data corresponds to a simulation with $k_{\text{off}} = k_{\text{on}} = \alpha = 1.0$. B) Plotting the maximum possible mutual information $I(X; Z)$ for $N = 100,000$ reveals that the maximum mutual information closely matches the entropy $H(X)$ at this N , shown by the agreement between the solid black line and dashed blue line. This suggests that when $N = 100,000$, one can infer the state of the upstream with a very high accuracy.